Cancer Letters 521 (2021) 14–28

Contents lists available at ScienceDirect

Cancer Letters

journal homepage: www.elsevier.com/locate/canlet

Inhibition of RAC1 activity in cancer associated fibroblasts favours breast tumour development through IL-1β upregulation

Angélica Martínez-López [a,b], Ana García-Casas [a,c], Paloma Bragado [c,d], Akira Orimo [e], Eduardo Castañeda-Saucedo [b], Sonia Castillo-Lluva [a,c,*]

[a] Departamento de Bioquímica y Biología Molecular, Facultad de Ciencias Químicas y Biológicas, Universidad Complutense, Madrid, 28040, Spain
[b] Laboratorio de Biología Celular del Cáncer, Facultad de Ciencias Químico-Biológicas, Universidad Autónoma de Guerrero, Mexico
[c] Instituto de Investigaciones Sanitarias San Carlos (IdISSC), Madrid, 28040, Spain
[d] Departamento de Bioquímica y Biología Molecular, Facultad de Farmacia, Universidad Complutense, Madrid, 28040, Spain
[e] Department of Pathology and Oncology, Juntendo University School of Medicine, Tokyo, Japan

ARTICLE INFO

Keywords:
Stromal RAC1
Cancer-associated fibroblasts
Breast cancer
IL-1β

ABSTRACT

Cancer-associated fibroblasts (CAFs) are highly abundant stromal components in the tumour microenvironment. These cells contribute to tumorigenesis and indeed, they have been proposed as a target for anti-cancer therapies. Similarly, targeting the Rho-GTPase RAC1 has also been suggested as a potential therapeutic target in cancer. Here, we show that targeting RAC1 activity, either pharmacologically or by genetic silencing, increases the pro-tumorigenic activity of CAFs by upregulating IL-1β secretion. Moreover, inhibiting RAC1 activity shifts the CAF subtype to a more aggressive phenotype. Thus, as RAC1 suppresses the secretion of IL-1β by CAFs, reducing RAC1 activity in combination with the depletion of this cytokine should be considered as an interesting therapeutic option for breast cancer in which tumour cells retain intact IL-1β signalling.

1. Introduction

Breast cancer (BC) is the most frequent cancer in women and it remains a major cause of cancer-associated death worldwide [1]. BC is a complex and heterogeneous disease with quite varied morphological manifestations, molecular features, behaviours and responses to therapy [2]. Cancer metastasis and resistance to treatment are two major causes of the poor survival of BC patients. Thus, understanding the molecular mechanisms that underlie metastasis will improve treatment regimens and ultimately, prognostic outcomes.

The GTPase RAC1 (Ras-Related C3 Botulinum Toxin Substrate 1) is a molecule that has been implicated in cancer progression and the poor prognosis of various tumour types [3,4]. RAC1 is a member of the Rho family of small GTPases that binds to either GTP or GDP, the exchange of which controls its activation. RAC1 is inactive in the GDP-bound state and it is activated upon exchange of its GDP for GTP, enabling downstream signalling to proceed [5]. The tumour microenvironment (TME) also influences cancer progression and it is defined by multiple cell types, such as fibroblasts, leukocytes, adipocytes, myoepithelial and endothelial cells. Moreover, the TME also contains soluble factors and extracellular matrix components (ECM) that shape the physical and chemical properties of tissues [6–8]. Fibroblasts are the most abundant cell type in the tumour-associated stroma, also known as cancer-associated fibroblasts (CAFs). CAFs can contribute to the malignant phenotype of tumour cells through a variety of mechanisms, including growth factor secretion, angiogenesis induction or ECM remodelling [9–12].

The expression of several markers can be used to differentiate CAFs from normal fibroblasts (NFs), such as alpha smooth muscle actin (αSMA), fibroblast activating protein (FAP), integrin β1/CD29, fibroblast specific protein (FSP1/S100-A4), platelet derived growth factor receptor β (PDGFRβ) and Caveolin-1 (CAV1). However, not all of these markers are expressed simultaneously by CAFs, contributing to the heterogeneity of CAFs in BC [13–15]. Using six CAF markers, four different CAF subpopulations were recently identified in breast and ovarian cancer, referred to as CAF-S1 to CAF-S4 [14,17]. The CAF-S1 and CAF-S4 subsets are detected at high levels in aggressive BC subtypes, such as HER2 (28.2% S1 and 61.8% S4) and Triple negative breast cancer (TNBC: 38% S1 and 42% S4), with the CAF-S1 subtype associated with distant relapse [16]. Alternatively, the CAF-S2 subset is enriched in

* Corresponding author. Departamento de Bioquímica y Biología Molecular, Facultad de Ciencias Químicas y Biológicas, Universidad Complutense, Madrid, Spain.
E-mail address: sonica01@ucm.es (S. Castillo-Lluva).

https://doi.org/10.1016/j.canlet.2021.08.014
Received 9 April 2021; Received in revised form 11 August 2021; Accepted 14 August 2021
Available online 19 August 2021

luminal BC (14.4% S1, 42% S2 and 29.8% S4) and CAF-S3 fibroblasts accumulate in healthy tissues [16,17].

RAC1 has been shown to control the shape, and the mechanical and adhesive properties of fibroblasts, as well as their capacity to organize the ECM and myofibroblast formation [18–20]. Because RAC1 is involved in malignant transformation, influencing tumorigenesis, angiogenesis, invasion and metastasis [21], we wondered if RAC1 activity could participate in CAF signalling to promote tumour development. In the present study, and contrary to our expectations, we found that RAC1 activity in CAFs is relevant to prevent the malignant phenotype of BC cells. Thus, the inhibition of RAC1 alters the CAF secretome, inducing IL-1β secretion that in turn enhances the aggressiveness of BC cells. Indeed, RAC1 inhibition in CAFs promotes a change in their phenotype, making them more aggressive. These results identify a novel role for RAC1 in the BC microenvironment that may be crucial for disease management.

2. Materials and methods

2.1. Reagents

EHop-016 (#SML0526-5 MG), Crystal Violet (#C3886) and recombinant SDF-1 (#SRP3276) were purchased from Sigma-Aldrich (St Louis, MO). The fibroblasts cell lines were transfected with siRNAs using DharmaFECT 2001 (Dharmacon, Lafayette, CO; #T2001), and the RAC1 siRNA (#sc-36351) and IL-1β siRNA (#sc-39616) were obtained from Santa Cruz Biotechnology (Heidelberg, Germany). The IL-1β neutralizing antibody was purchased from InvivoGen (#mabg-hil1b-3).

2.2. Human CAF isolation

To establish the non-tumour associated NF cell line, we obtained fresh healthy mammary tissue from a woman undergoing reduction mammoplasty [22]. CAFs from the Luminal-HER2$^+$ and TNBC cell lines were established from tumour tissue excised from breast cancer patients: a Luminal B-HER2$^+$ patient and TNBC patients [23]. These fibroblasts (NFs and CAFs) were immortalized by infection with the pMIG (MSCV-IRES-GFP) retroviral vector, expressing both hTERT and GFP, and with a pBabe-puro vector encoding a puromycin resistance gene, before they were co-implanted with breast carcinoma cells into nude mice to generate Lum-CAFs [22].

2.3. Cell culture

NFs and CAFs [22,23] were grown in complete DMEM containing 4.5 g/l glucose and L-glutamine (Sigma Aldrich) in the presence of calf serum (10%). MDA-MB-231 and MCF-7 cells (ATCC) were grown in complete DMEM containing 4.5 g/l glucose and L-glutamine (Sigma Aldrich). BT-474 and T-47D cancer cells were grown in RPMI medium. In all cases, the medium was supplemented with 56 IU/ml penicillin, 56 mg/l streptomycin (Invitrogen, Carlsbad, CA) and 10% foetal bovine serum (FBS: LINUS #16sV30180.03), and the cells were maintained at 37 °C in a humid atmosphere containing 5% CO_2. All cells were routinely tested for mycoplasma contamination. The cell lines were analysed for authentication at the Genomics Core Facility at the Instituto de Investigaciones Biomédicas "Alberto Sols" (CSIC-UAM, Madrid, Spain) using STR PROFILE DATA, the STR amplification kit (GenePrintR 10 System, Promega), STR profile analysis software GeneMapper® v3.7 (Life Technologies) and a Genomic Analyzer System ABI 3130 XL (Applied Biosystems).

2.4. Transfection experiments

For siRNA transfection experiments, a pool of constructs was used that specifically targeting *RAC1* (Santa Cruz Biotechnology, sc-36351) or *IL-1β* (sc-39616) and a control siRNA (sc-37007). In general, 1 × 10^6 cells were transfected using the DharmaFECT 1 Transfection Reagent (Dharmacon catalogue number T-2001) and incubated for up to 72 h before starting the experiment. For plasmid transfection experiments, 5 μg of plasmids pEGFP-RAC wild type (WT), pEGFP-RAC constitutively active (V12) or pEGFP-C3 (empty vector) was used [24]. Cells were transfected using Lipofectamine 2000 (Invitrogen, #11668–027) and incubated for 24 h before starting the experiments.

2.5. Conditioned media

The CAFs and NFs were grown for three days in the absence of serum, and the culture supernatants were collected and used as conditioned medium (CM) in proliferation, migration, invasion and RAC1 activity experiments. For RAC1 inhibition, CAFs were treated with EHop-016 (5 μM) for 24 h, a concentration at which RAC1 is selectively inhibited [25]. The medium was then removed and the cells were grown for two days in the absence of serum. For inhibition of IL-1β with the neutralizing antibody, the IL-1β antibody (40 ng/mL) or an isotype control were incubated with the CAFs for 24 h in the previously collected CM. The supernatant recovered was filtered to remove unattached cells and cell debris.

2.6. Protein analysis

Proteins were analysed in western blots as described previously [26]. In brief, proteins were extracted from the tumours in FISH buffer [Glycerol 100X, 1 M Tris pH 7.4, 5 M NaCl, 1% (v/v) NP40 and 1 M $MgCl_2$], while the proteins from the cell lines were extracted in TNES buffer [100 mM NaCl, 1% (v/v) NP40, 50 mM Tris-HCl pH 7.6, 20 mM EDTA], both containing protease and phosphatase inhibitor cocktails (Sigma-Aldrich; #P8340). The proteins recovered were quantified using a Bradford Protein Assay (Bio-Rad #5000006), resolved by SDS-PAGE on 10–12% gradient gels (purchased from Bio-Rad, Berkeley, CA; #456–8085) and transferred to polyvinylidene difluoride membranes (Immobilon-P, Millipore, Burlington, MA). The membranes were then probed with the following primary antibodies: anti-RAC (1:1000, clone 102: BD Biosciences, Franklin Lakes, NJ), anti-Cyclin D1 (1:1000, #sc8396: Santa Cruz Biotechnology), anti-Tubulin (1:1000, DM1A: Sigma-Aldrich; #T6199), anti-GAPDH (1:1000, #G8795: Sigma-Aldrich), anti-GFP (1:1000 SAB4301795, Sigma-Aldrich), anti--Laminin (1:1000, #7292: Santa Cruz Biotechnology), anti-HSP90 (1:1000, #515081: Santa Cruz Biotechnology), anti-pERK 1/2 (1:1000, #9101: Cell signalling), anti-ERK total (1:1000, #4696: Cell signalling), anti-pAKT S473 (1:1000, #32581: Elabscience), anti-AKT total (1:1000, #30471: Elabscience), anti-p65 (1:1000, #372: Santa Cruz Biotechnology). Antibody binding was detected with horseradish peroxidase (HRP)-conjugated anti-mouse, anti-rabbit or anti-sheep secondary antibodies (1:10,000 dilution: Bio-Rad), and visualized by enhanced chemiluminescence (ECL, # 170–5061: Bio-Rad). The images were obtained with the ImageQuant LAS 500 chemiluminescence CCD camera (GE Healthcare Life Sciences, Chicago, Illinois, USA).

2.7. Cell viability

MDA-MB-231 cells were plated for 24, 48 and 72 h, at which point they were fixed for 10 min in PBS with 4% paraformaldehyde at room temperature and stored in PBS with 0.05% azide at 4 °C prior to staining with crystal violet for 30 min at room temperature. The plates were washes with tap water and the crystal violet was removed from the cells with 1% Triton X-100 in PBS, measuring their OD at 570 nm.

2.8. RAC1 GTPase assay

The endogenous active GTP-bound RAC1 was measured using a GST-PAK1 binding domain (PBD) pull-down assay. Cells were lysed in FISH buffer [Glycerol 100X, 1 M Tris pH 7.4, 5 M NaCl, 1% (v/v) NP40 and 1

M $MgCl_2$] and equal volumes were incubated with GST-PBD beads (20 μg) for 15 min at 4 °C. The complexes precipitated were washed three times with excess lysis buffer and after the final wash, the supernatant was discarded and the beads were suspended in 10 μl of 5X Laemmli sample buffer. GTP-bound RAC1 was detected in western blots and the amount of GTP-bound RAC1 was normalized to the total amount of this GTPase in cell lysates for each sample.

2.9. Boyden chamber cell migration/invasion assay

Cell migration was assayed in Boyden chambers (8.0 μm pore-size polyethylene terephthalate membrane with a cell-culture insert: VWR, Radnor, PA; #VWRI734-2744). The cells were trypsinised and counted, and cell suspensions containing 5×10^4–1 $x10^5$ cells in 200 μl of serum-free medium were added to the upper chamber, with 500 μl of the appropriate medium added to the lower chamber. The transwell inserts were incubated at 37 °C for 24 h with MDA-MB-231 cells or 48 h with BT-474 cells, after which the cells on the inside of the transwell inserts were removed with a cotton swab while those on the underside of the insert were fixed and stained. Photographs were taken of five random fields per insert and the cells were counted to calculate the proportion of transmigrated cells. Boyden chambers with 0.7 mg/ml of matrigel (Cell Biolabs, San Diego, CA; #CBA-110) and 1.5×10^5 cells were used to assay cell invasion.

2.10. Wound assays

MCF-7 and T-47D cells were grown to confluence and overnight with 0% FBS. The cell monolayer was scraped in a straight line with a pipette tip in order to create a linear wound. Debris were removed by washing the cells with PBS and then replaced with CM. Photographs of the wounds (at least 3 fields per condition) were taken with a NIKON TMS microscope with a 10X objective. For each image cells migrated into the original wound were measured. The migration area was determined by measuring the total area of the wound using the ImageJ software.

2.11. Gelatin zymograms

To assess the activity of the metalloproteases MMP-2 and MMP-9, the CM from CAFs was collected. The protein concentration was determined by the Bradford method and CM for each condition containing 40 μg of protein was assayed for proteolytic activity on gelatin-substrate gels. Briefly, samples were mixed with non-reducing buffer containing 2.5% SDS and separated in 8% acrylamide gels co-polymerized with gelatin (1 mg/mL), as described previously [29]. After electrophoresis at 72 V for 2.5 h, the gels were rinsed twice in 2.5% Triton X-100, and then incubated at 37 °C for 24 h in 50 mM Tris-HCl (pH 7.4 to MMP-2 or pH 8.3 to MMP-9) and 5 mM $CaCl_2$ assay buffer. The gels were fixed and stained with 0.25% Coomassie Brilliant Blue G-250 in 10% acetic acid and 30% methanol. Proteolytic activity was detected as clear bands against the background stain of undigested substrate in the gel and it was quantified using ImageJ software (NIH, Bethesda, MD, USA).

2.12. Immunofluorescence microscopy

Cells were plated and grown on glass coverslips for 48 h, fixed for 10 min with 4% paraformaldehyde (PFA) at room temperature and the coverslips were then stored in PBS with 0.05% sodium azide at 4 °C until the cells were immunostained. Briefly, the cells were permeabilised by incubating for 3 min at 4 °C in PBS containing 0.5% Triton X-100 and then, the coverslips were incubated overnight at 4 °C with a 1:200 dilution of the primary antibody against Ki67 (Thermo Fisher Scientific, #PA1-21520). After rinsing thoroughly, the coverslips were incubated with Alexa Fluor 488 or 594 goat anti-mouse-IgG or anti-rabbit-IgG secondary antibodies (Invitrogen), counterstained with DAPI for 30 s, and then mounted on glass slides with DAPI using the Gold antifade reagent (Invitrogen; #P36935). Immunofluorescence was analysed under a Zeiss microscope (Zeiss Axioplan 2).

To calculate the proliferation ratio using the Ki67 marker, we counted the total number of positively stained tumour cells in each image/field and the total number of tumour cells in each image. The percentage of Ki67 positive cells was calculated as: No. of positive tumour cells/total No. of tumour cells × 100.

2.13. Quantitative real time PCR (qPCR)

Total RNA was isolated from cells with the RNAeasy Mini kit (QIAGEN) according to the manufacturer's instructions and quantified using a NanoDrop® Spectrophotometer. RNA (3 μg) was reverse transcribed in a final volume of 20 μL using a NZY First-Strand cDNA Synthesis Kit (NZYTech) following the manufacturer's instructions. To determine the *RAC1, SMA, FAP, SDF-1, IL-1β, IL-8, CD29, CAV1, PDGFRβ1, FSP1, IL1R, IL1RA* and *GAPDH* gene expression, the SYBR Green reagent was used in the PCR reaction mixture (10 μL final volume). The primers used were: *RAC1* F-CTGATGCAGGCCATCAAGT, R-CAGGAAATGCATTGGTTGTG; *SMA* F-GTGTGTGACAATGGCTCTGG, R-TGGTGATGATGCCATGTTCT; *FAP* F-*TGTGCATTGTCTTACGCCCT,* R-*CCGATCAGGTGATAAGCCGT; SDF-1* F-TGAGAGCTCGCTTTGAGTGA, R-CACCAGGACCTTCTGTGGAT; *IL-1β* F-CCACCTCCAGGGACAGGATA, R-AACACGCAGGACAGGTACAG: *IL-8* F-ACTGAGAGTGATTGAGAGTGGAC, R- AACCCTCTGCACCCAGTTTTC; *CD29* F-TTTGTTTAATGTCTGGTGCTTTCTG R-CCCCAAAATTGCAAACAAATACA; *PDGFRβ* F-ACACGGGAGAATACTTTTGC, R-GTTCCTCGGCATCATTAGGG; *CAV1* F-GAGCTGAGCGAGAAGCAAGT, R-CAAATGCCGTCAAAACTGTG; *FSP1* F-GATGAGCAACTTGGACAGCAA, R-CTGGGCTGCTTATCTGGGAAG; *IL1R* F-AGAGGAAAACAAACCCACAAGG, R-CTGGCCGGTGACATTACAGAT; *IL1RA* F-AACAGAAAGCAGGACAAGCG, R-CCTTCGTCAGGCATATTGGT and *GAPDH* F-CTGCACCACCAACTGCTTAG, R-GTCTTCTGGGTGGCAGTGAT. PCR was performed on Fast Real-Time PCR System (Applied Biosystems) and the transcript levels were normalized to those of GAPDH, which was used as an endogenous control. Gene expression was analysed in triplicate and were quantified using the $^{\Delta\Delta}$Ct method.

2.14. Secretome analysis

The levels of 36 human cytokines in the supernatant were measured using the Proteome Profiler Human Cytokine Array (R&D Systems), a membrane-based immunoarray, according to the manufacturer's instructions. Immediately after addition of the chemiluminescence substrate, the immunoblots were captured with the ImageQuant LAS 500 chemiluminescence CCD camera (GE Healthcare Life Sciences, Chicago, Illinois, USA). The cytokine expression in each sample was determined by spot densitometry using the ImageJ software (NIH, USA), correcting for background by subtracting the mean optical density of negative control spots on each immunoblot.

2.15. Enzyme-linked immunosorbent assay (ELISA)

To detect secreted IL-1β and IL-8 in the CM of cultured CAFs, the medium was concentrated using Amicon Ultra-15 Centrifugal Filter Units with an Ultracel-10 membrane (Merck Millipore, UFC901024), and ELISA was carried out using Human IL-1β/IL-1F2 DuoSet ELISA (DY201) and Human IL-8/CXCL8 DuoSet ELISA (DY208) according to the manufacturer's instructions (R&D Systems).

2.16. Chicken embryo experiments

In vivo experiments using chicken embryos do not require any special permits as long as the embryos are sacrificed before hatching, as occurred in this study. For the CAM xenografts we used premium specific pathogen-free (SPF), fertile, day 11 fertilised chicken eggs. We co-

inoculated 1 × 10^6 MDA-MB-231 cells expressing the green fluorescent protein (GFP) or T-47D cells, alone or together with CAFs previously treated with the RAC1 inhibitor, EHop-016 (ratio 1:1, diluted in PBS and matrigel), allowing the tumours to grow for seven days. The tumour cells were injected into the chicken embryo, placing them in the middle of a small sterile plastic ring that prevents the diffusion of any treatments administrated to the areas surrounding the tumour. The tumours were treated with an IL-1β neutralizing antibody (100 ng/mL) or a Rac inhibitor (0.5 μM, EHop-016) 4 and 6 days after inoculation, as necessary. After seven days the tumours and lungs were excised, weighed and measured, and immediately fixed overnight in 4% PFA at room temperature and washed in 70% EtOH before their inclusion in paraffin. Sections (3 μm) were deparaffinised and processed for immunofluorescence staining.

2.17. Quantitative detection of human tumour cell metastasis

Human tumour cells were detected in chicken lungs based on the quantitative detection of human Alu sequences in chicken lung DNA extracts, a modification of the method developed by Kim et al. [27]. Briefly, the lungs were snap frozen in liquid nitrogen and the genomic DNA was extracted using proteinase K, analysing the genomic DNA (30 ng) in PCR reactions. To detect human cells in the chick tissues, primers specific for the human *Alu* sequences (F-ACGCCTGTAATCCCAGCACTT; and R-TCGCCCAGG CTGGAGTGCA) were used to amplify the human Alu repeats present in the genomic DNA extracted from the chicken tissues. Amplification of chicken *Gapdh* (*chGapdh*: F- GAGGAAAGGTCGCCTGGTGGATCG and R- GGTGAGGACAAGCAGTGAGGAACG) was used as an internal control for the total amount of tissue.

2.18. Statistical analyses

Unless otherwise indicated, the data are expressed as the mean ± standard error of the mean (s.e.m.) and evaluated with a Mann–Whitney *U* test (non-parametric) or *t*-test (parametric) for two groups, or with the Kruskal–Wallis test (followed by Dunn's multiple comparison post-test) or by ANOVA (followed by Turkey's multiple comparisons test) when more than two groups were compared. The percentage of positive cells was evaluated using the χ^2 test and the tumour volumes in the mice were compared using a multiple *t*-test. For all the analyses, *P*-values ≤0.05 were considered statistically significant.

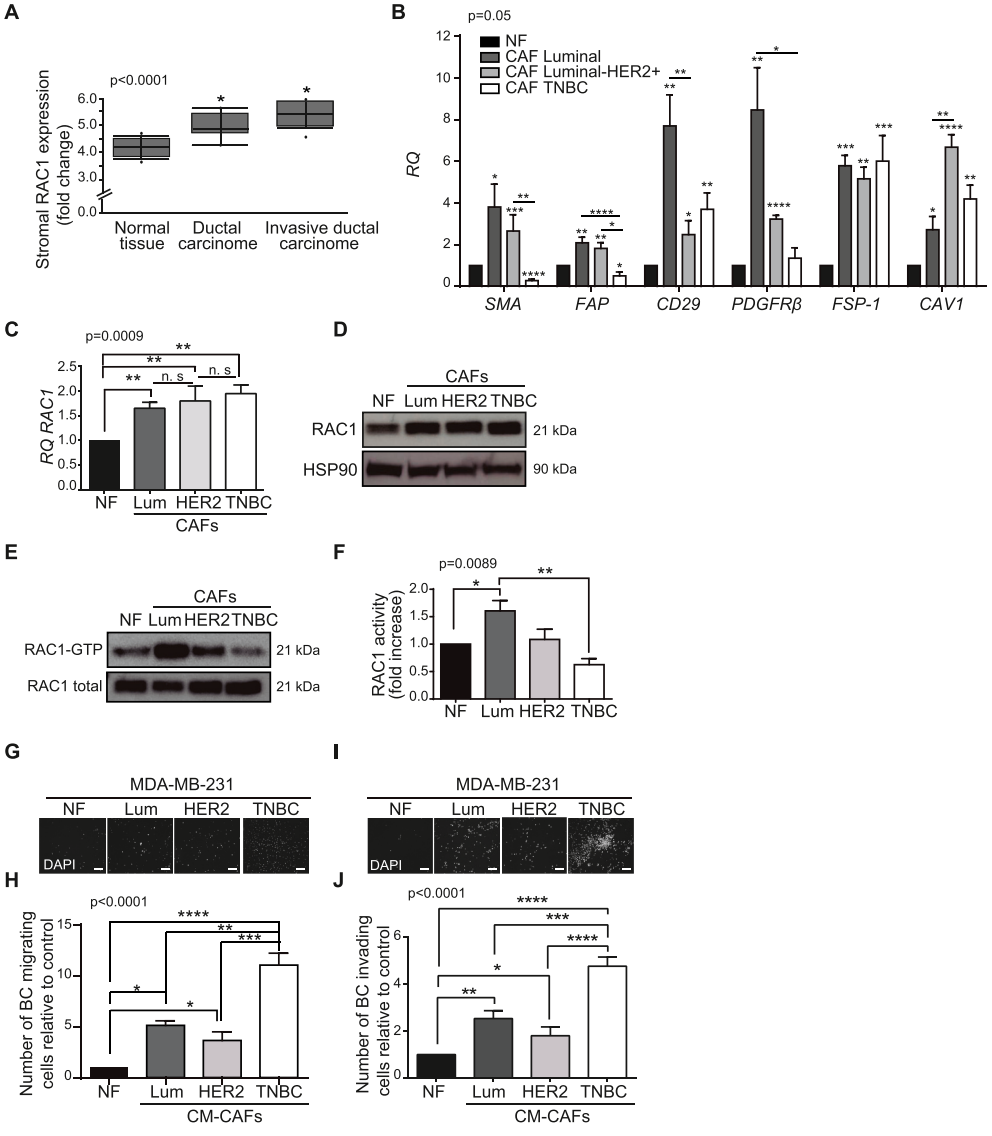

Fig. 1. RAC1 activity in the stroma compartment influences breast cancer evolution. (A) Analysis of RAC1 mRNA expression in the Oncomine database. RAC1 expression in normal breast stromal tissue, and that derived from ductal and invasive carcinoma relative to control samples (p = 2.53 E−4). (B) Expression of CAF markers in CAFs of different molecular BC subtypes (ANOVA test; Tukey's post-hoc test). (C) RAC1 mRNA levels determined by RT-qPCR. RQ, relative quantification normalized to NFs (ANOVA test; Tukey's post-hoc test). (D) Representative Western blot of RAC1 protein from different CAF subtypes. Lum (Luminal), HER2+ (Luminal-HER2+) and TNBC (Triple negative breast cancer). (E) Representative Western blot of active RAC1 in different CAF subtypes. (F) Densitometry of active RAC1 from D, quantifying the data from at least three independent experiments with ImageJ software (ANOVA test; Tukey's post-hoc test). (G, H) Transwell migration assays, shown as the number of migrating BC cells relative to conditioned medium (CM) from NFs. Representative images of MDA-MB-231 migrated cells stained with DAPI (G) and (H) quantification of the number of migrating cells relative to the controls (ANOVA test; Tukey's post-hoc test). (I, J) Matrigel invasion assay, shown as the number of invading BC cells relative to that induced by the CM from NFs. (I) Representative images of MDA-MB-231 invasive cells stained with DAPI. (J) Quantification of the number of invading cells relative to the control (ANOVA test; Tukey's post-hoc test). Scale bar: 200 μm. The data are the mean ± SEM (n ≥ 3) and the statistical differences between the groups indicated are denoted as *P ≤ 0.05; **P ≤ 0.01.

3. Results

3.1. RAC1 activity in the stroma compartment influences breast cancer progression

Overexpression of RAC1, together with deregulation of RAC1 regulators, has been considered the main perturbation to RAC1 signalling in cancer [28]. There is considerable evidence that enhanced Rho protein expression, including that of RAC1, is associated with tumour formation, growth and progression, an indication of the positive contribution of increased Rho GTPase activity to tumorigenesis [21]. However, the influence of RAC1 activity on CAF signalling to promote tumour development has not yet explored. To assess the prognostic influence of RAC1 in the stroma of BC, a bioinformatics analysis was performed on a public human stromal BC dataset (GSE14548) [29], revealing that *RAC1* expression in the stroma of ductal carcinomas was significantly stronger

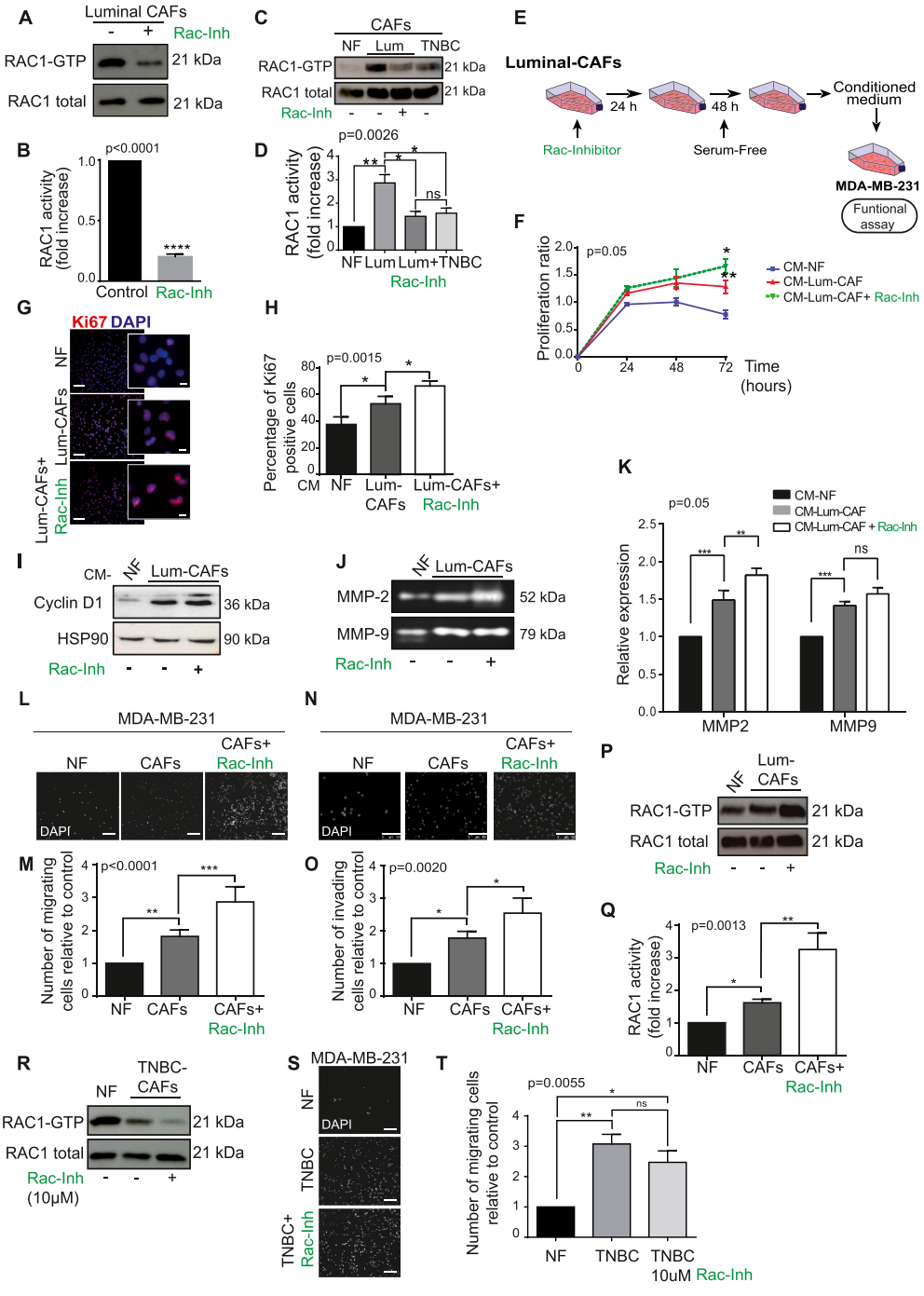

Fig. 2. The inhibition of RAC1 activity in luminal CAFs disturbs the oncogenic activity of breast cancer cells. (A) RAC1 activity in luminal CAFs exposed to the Rac-inhibitor EHop-016 (5 μM). (B) Quantification of the relative normalized amounts of RAC–GTP in A, as determined by scanning densitometry (*t*-test). (C) Representative Western blot of RAC1 activity in the CAFs indicated. (D) Quantification of the relative normalized amounts of RAC–GTP in C, as determined by scanning densitometry (ANOVA test; Tukey's post-hoc test) (E) Schematic representation of the experimental design to collect conditioned medium (CM) from CAFs. (F) The MDA-MB-231 BC cell line was treated with CM from the indicated fibroblasts and cell viability was assessed with crystal violet staining (2way ANOVA test; Sidak's post-hoc test). (G) Representative image of immunofluorescent evaluation of Ki-67 expression in MDA-MB-231 BC cells and (H) the percentage of Ki-67-positive cells ($\chi 2$ test). (I) Cyclin D1 expression in MDA-MB-231 cells treated with CM from the indicated fibroblasts. (J) Representative zymogram gels corresponding to the degradation bands of MMP-9 and MMP-2. (K) Band quantification from gelatin zymography in H as determined by scanning densitometry (ANOVA test; Tukey's post-hoc test). (L) Representative images of MDA-MB-231 cell migration determined in Boyden chambers. (M) Migrating cells were determined as the number of migrating cells relative to the CM from NFs (ANOVA test; Tukey's post-hoc test). (N) Representative images of cell invasion assessed in a Matrigel invasion assay. (O) Invading cells were determined as the number of invading cells relative to the CM from NFs (ANOVA test; Tukey's post-hoc test). (P) Representative Immunoblotting of RAC1 activity in the MDA-MB-231 BC cell line stimulated with the indicated CM. (Q) Quantification of the relative normalized amounts of RAC–GTP in P as determined by scanning densitometry (ANOVA test; Tukey's post-hoc test). (R) Representative Western blot of RAC1 activity in TNBC CAFs treated with Rac inhibitor (10 μM). (S) Representative images of MDA-MB-231 cell migration determined in Boyden chambers. (T) Migrating cells were determined as the number of migrating cells relative to those seen with NF CM (ANOVA test; Tukey's post-hoc test). Scale bar: 200 μm. The data are the mean ± SEM ($n \geq 3$) and the statistical differences between the groups indicated are denoted as: *P ≤ 0.05; **P ≤ 0.01. (For interpretation of the references to colour in this figure legend, the reader is referred to the Web version of this article.)

than in the normal stroma. Indeed, these differences were more significant when compared with the stroma of invasive ductal carcinoma (Fig. 1A) and importantly, similar results were obtained when the epithelial compartment was analysed (Fig. S1A).

To rule out the influence of RAC1 activity in CAFs to support the growth and progression of carcinoma cells, we examined CAFs of different molecular subtypes obtained from BC patients (see Materials & Methods for details) [22,23]. First, we confirmed that the expression of different markers was up-regulated in the CAFs selected, such as α-SMA, FSP1, PDGFRβ, CAV1, CDC29 and FAP that are all involved in the malignancy of different tumours (Fig. 1B) [13]. Accordingly, RAC1 was more strongly expressed in the CAFs from each of the molecular BC subtypes studied than in NF, yet no differences were observed between each CAF subtype (Fig. 1C and D).

RAC1 is inactive in its GDP-bound state and it is activated by exchanging GDP for GTP, triggering downstream signalling. When the activity of RAC1 (RAC1-GTP) was analysed in the different CAFs it was seen to diminish as tumours became more aggressive (Fig. 1E and F). Moreover, to confirm that RAC1 activity could affect tumour behaviour, the migratory capacity of the MDA-MB-231 human BC cell line stimulated with CM obtained from the different CAFs was analysed. Interestingly, lower RAC1 activity in CAFs was related to a higher migratory (Fig. 1G, **H**) and invasive (Fig. 1I, **J**) capacity of MDA-MB-231 BC cells. Moreover, the CM from CAFs appeared to induce the migration of Luminal MCF7 BC cells or Luminal-HER2^{+} BT-474 cells (Figs. S1B and C). These results suggest that the different levels of RAC1 activity in CAFs and not the total RAC1 could influence BC cell malignancy.

3.2. Inhibiting the RAC1 activity in luminal CAFs disturbs the oncogenic activity of breast cancer cells

As indicated, RAC1 activity in CAFs may inhibit the migratory and invasive capacity of BC cells. Thus, to evaluate the consequences of inhibiting RAC1 activity in CAFs, supporting the growth and progression of carcinoma cells, luminal CAFs that have high levels of active RAC1 (RAC1-GTP) (Fig. 1 and Fig. S2A-**D**) were exposed to a specific Rac inhibitor, EHop-016 (5 μM) [25]. Luminal CAFs exposed to the Rac inhibitor for 24 h reduced RAC1 activity by 80% (Fig. 2A, **B**), generating luminal fibroblasts with RAC1 activity similar to TNBC cells (Fig. 2C, **D**).

RAC1 inhibited cells were incubated in serum-free medium for 48 h to generate CM, which was used to treat MDA-MB-231 cells and to evaluate the implications of reducing RAC1 activity to similar levels as that in TNBC cells in terms of proliferation and migration/invasion (Fig. 2E). CM from CAFs (CAF-CM) promoted MDA-MB-231 proliferation relative to NF CM (NF-CM) and CM from CAFs treated with the Rac inhibitor strongly enhanced BC proliferation compared to CAF-CM (Fig. 2F). These results were corroborated by staining with the Ki-67 proliferative marker (Fig. 2G, **H**). Since Cyclin D1 is essential for BC cell proliferation [30], we evaluated its expression following exposure to the CM and in accordance with the previous results, the CM obtained from CAFs exposed to the Rac inhibitor strongly increased Cyclin D1 expression (Fig. 2I).

Mounting evidence suggests that extracellular proteinases like the matrix metalloproteinases (MMPs) may mediate many of the changes in the TME during tumour progression. Significantly, CAFs have been implicated in MMPs production [31] and this phenomenon could promote a pro-tumorigenic phenotype [32]. The MMP-2 and MMP-9 (gelatinase) activity in the supernatant from NFs, CAFs and Rac-inhibited CAFs was assessed, and only MMP-2 activity differed in the supernatant of CAFs exposed to the Rac inhibitor relative to the control CAF-CM, indicating that inhibiting RAC1 in CAFs upregulates MMP-2 but not MMP-9 secretion (Fig. 2J, **K**).

Finally, we assessed the effect of CM from NFs, CAFs and Rac-inhibited CAFs on tumour cell migration and invasion. As expected, CAF-CM enhanced tumour cell migration significantly more than NF-CM. However, the inhibition of RAC1 activity in CAFs produced a CM that more strongly stimulated MDA-MB-231 tumour cell migration than CAF-CM (Fig. 2L, **M**). Similar results were obtained for invasion (Fig. 2N, **O**) and indeed, the enhanced migration and invasion observed in MDA-MB-231 cells exposed to CM from Rac-inhibited CAFs correlated with the activation of the GTPase RAC1 in this BC cell line (Fig. 2P, **Q**). By contrast, inhibiting RAC1 activity in the TNBC CAFs, which have weak RAC1 activity, did not affect the migratory capacity of the MDA-MB-231 cells (Fig. 2R–**T** and **Fig. S2E**).

Together, these results suggest that inhibiting RAC1 activity in luminal CAF cells that have strong RAC1 activity drives the pro-tumorigenic effects of these CAFs on TNBC cells, which could in part explain how RAC1 activity in the stromal compartment influences BC evolution.

3.3. Inactivation of RAC1-GTP cause molecular changes in the CAF subtypes

The inhibition of RAC1 activity in luminal CAFs induces changes compatible with TNBC CAFs. Four CAF subsets have recently been characterized in BC (CAF-S1 to CAF-S4), each with different characteristics in terms of aggression and levels of activation [13,17]. Thus, we assessed if the inhibition of RAC1 activity affected the expression of the different CAF markers. CAF heterogeneity in human BC has been defined according to the expression of six fibroblast markers, including FAP, CD29, αSMA, FSP1, PDGFRβ and CAV1 [13]. We found changes in the expression of four of these markers upon RAC1 inhibition in luminal CAFs, and while FAP and PDGFRβ expression was upregulated, CD29 expression was downregulated (Fig. 3A).

We hypothesized that RAC1 inactivation in luminal CAFs that expressed markers compatible with the S4-like subtype drives changes in this subset of markers, inducing a S1-like subtype more characteristic of TNBC CAF (Fig. 3B). To confirm that RAC1 activity was required to maintain the less aggressive CAF phenotype (S4-like), we compared the functional characteristics of CAF S4-like (luminal CAFs) and RAC-inhibited CAFs with the TNBC CAFs (S1-like) that are more migratory and display enhanced cytokine signalling [13].

The inhibition of RAC1 activity promoted a more migratory (Fig. 3C, D) and invasive (Fig. 3E, F) phenotype in MDA-MB-231 cells, similar to that obtained with TNBC CAFs. Furthermore, to assess if RAC1 activity was required to prevent the pro-tumorigenic activity of CAFs, we transfected TNBC CAFs that have weak RAC1 activity with plasmids expressing GFP, GFP-tagged wild-type RAC1 (GFP–RAC1) or a constitutively active RAC1 mutant (GFP-RAC1V12) (Fig. 3G). The expression of GFP–RAC1V12 but not that of GFP–RAC1 reduced the migratory capacity of these BC cells upon exposure to CM (Fig. 3H-I).

Together, these results suggest that the inhibition of RAC1 activity in luminal CAFs induced pro-tumorigenic changes in a shift towards TNBC subtype of CAFs. By contrast, overexpression of the active form of RAC1 reduced the pro-tumorigenic activity of TNBC CAFs. Thus, RAC1 activity could be considered an inhibitor of the oncogenic characteristics of CAFs.

3.4. Genetic RAC1 depletion is sufficient to induce the pro-tumorigenic activity of CAFs

To confirm the effects of the Rac inhibitor on CAFs, and that the effects of the CM derived from these cells were RAC1 specific and not an off-target effect, CAF cells were treated with a specific pool of siRNAs to deplete RAC1 over 96 h, assessing the CM obtained in functional assays on MDA-MB-231 cells (Fig. 4A-C). As occurred with CM from Rac1-inhibited CAFs (Fig. 2), the CM from *RAC1*-depleted CAFs increased the proliferation of the MDA-MB-231 cells, measured with the Ki67 marker (Fig. 4D, E), as well as their migratory and invasive capacity (Fig. 4F-I), and their MMPs secretion (Fig. 4J and K). Moreover, *RAC1* silencing reduced the overall RAC1 activity in CAFs (Fig. 4L, M) and therefore, the resulting CM increased the RAC1 activity in the stimulated

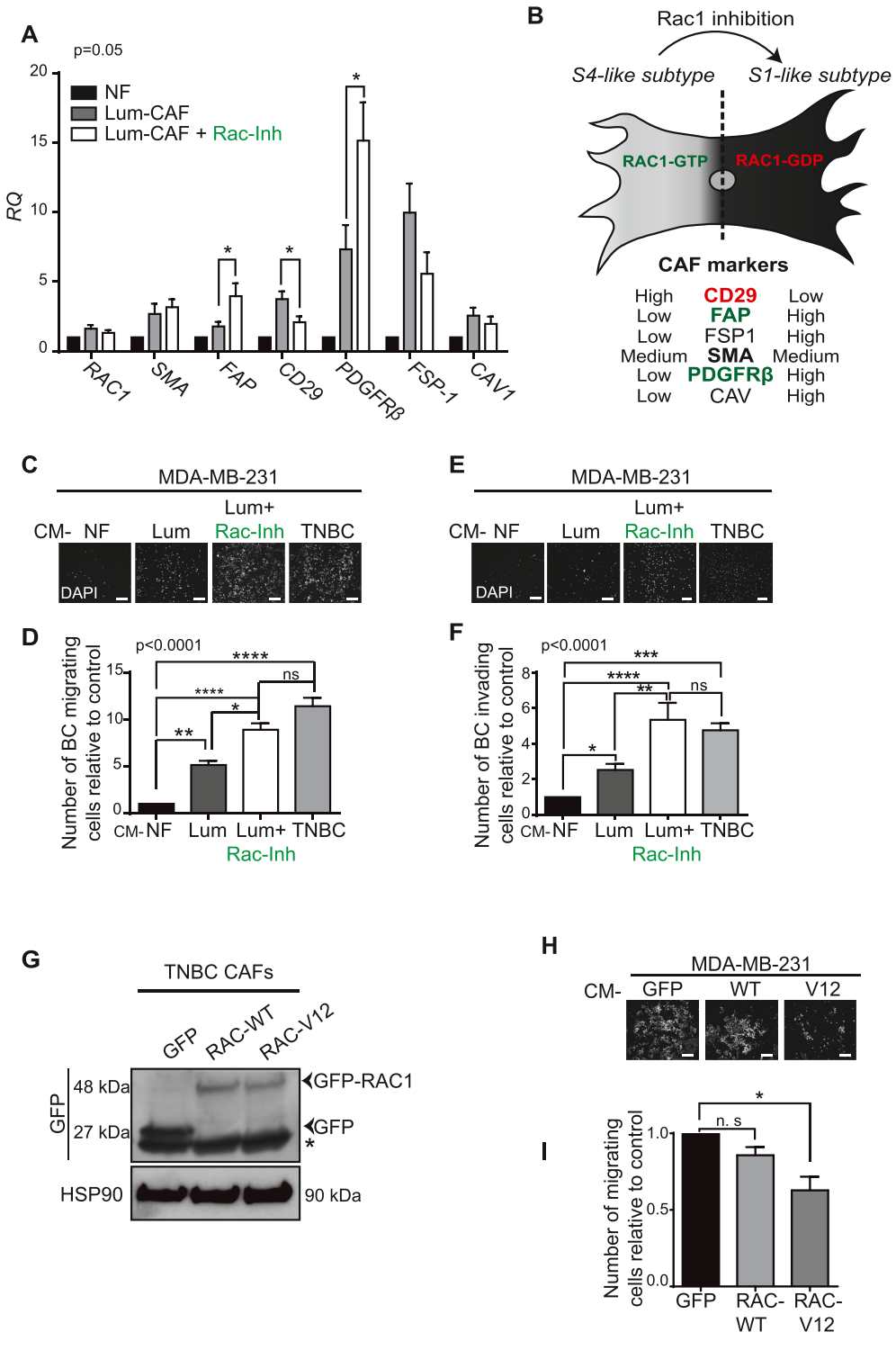

Fig. 3. Inactivation of RAC1 cause molecular changes in the CAF subtypes. (A) Expression of CAF markers in NFs and luminal CAFs treated with the RAC1 inhibitor by RT-qPCR in at least 3 different experiments (ANOVA test; Tukey's post-hoc test). RQ, relative quantification normalized to control. (B) Model showing the changes in CAF markers in response to RAC1 inactivation that promotes the S1-like subtype. (C) Representative images of migrating MDA-MB-231 cells stained with DAPI. (D) Cell migration was assayed in Boyden chambers as the number of MDA-MB-231 cells treated with CM from CAFs that had migrated relative to those exposed to CM from NFs (ANOVA test; Tukey's post-hoc test). (E) Representative images of invading cells stained with DAPI. (F) Invasion was determined as the number of MDA-MB-231 cells treated with CM from CAFs relative to those exposed to CM from NFs (ANOVA test; Tukey's post-hoc test). (G) Representative Western blot of GFP, GFP-RAC1 and GFP-RACV12 expression in TNBC CAFs. Unspecific band (*) (H) Representative images of migrating MDA-MB-231 cells stained with DAPI. (I) Cell migration was assayed in Boyden chambers, quantified as the number of MDA-MB-231 cells treated with CM from CAFs that had migrated relative to those exposed to GFP CM (ANOVA test; Tukey's post-hoc test). Scale bar: 100 μm. The data are the mean ± SEM ($n \geq 3$) and the statistical differences between the groups indicated are denoted as: *$P \leq 0.05$, **$P \leq 0.01$, ***$P \leq 0.001$ and ****$P \leq 0.0001$.

MDA-MB-231 BC cell line (Fig. 4N, O). Furthermore, like the pharmacological inhibition of RAC1 activity (Fig. 3), we found changes in the expression of four fibroblast markers upon RAC1 depletion, and while FAP and PDGFRβ expression was upregulated, SDF-1 and CD29 expression was downregulated (Fig. 4P).

Collectively, these results suggest that inhibiting RAC1 in luminal CAFs through genetic or pharmacological approaches increases the protumorigenic activity of CAFs.

3.5. Inhibition of RAC1 activity alters cytokine production by CAFs

Since CAFs stimulate tumour cell migration through the secretion of different cytokines into the TME, and the dissemination of TNBC cells is altered by exposing them to CM from Rac-inhibited luminal CAFs, we wondered if RAC1 might suppress the production of cytokines by CAFs. Differences in the production of some cytokines were evident in antibody arrays of the CAFs treated with the Rac inhibitor (Fig. 5A and Fig. S3A). Accordingly, there was less SDF-1 (CXC12) and ICAM-1 in the supernatant of these CAFs, and minor changes in IFN-γ. However, we

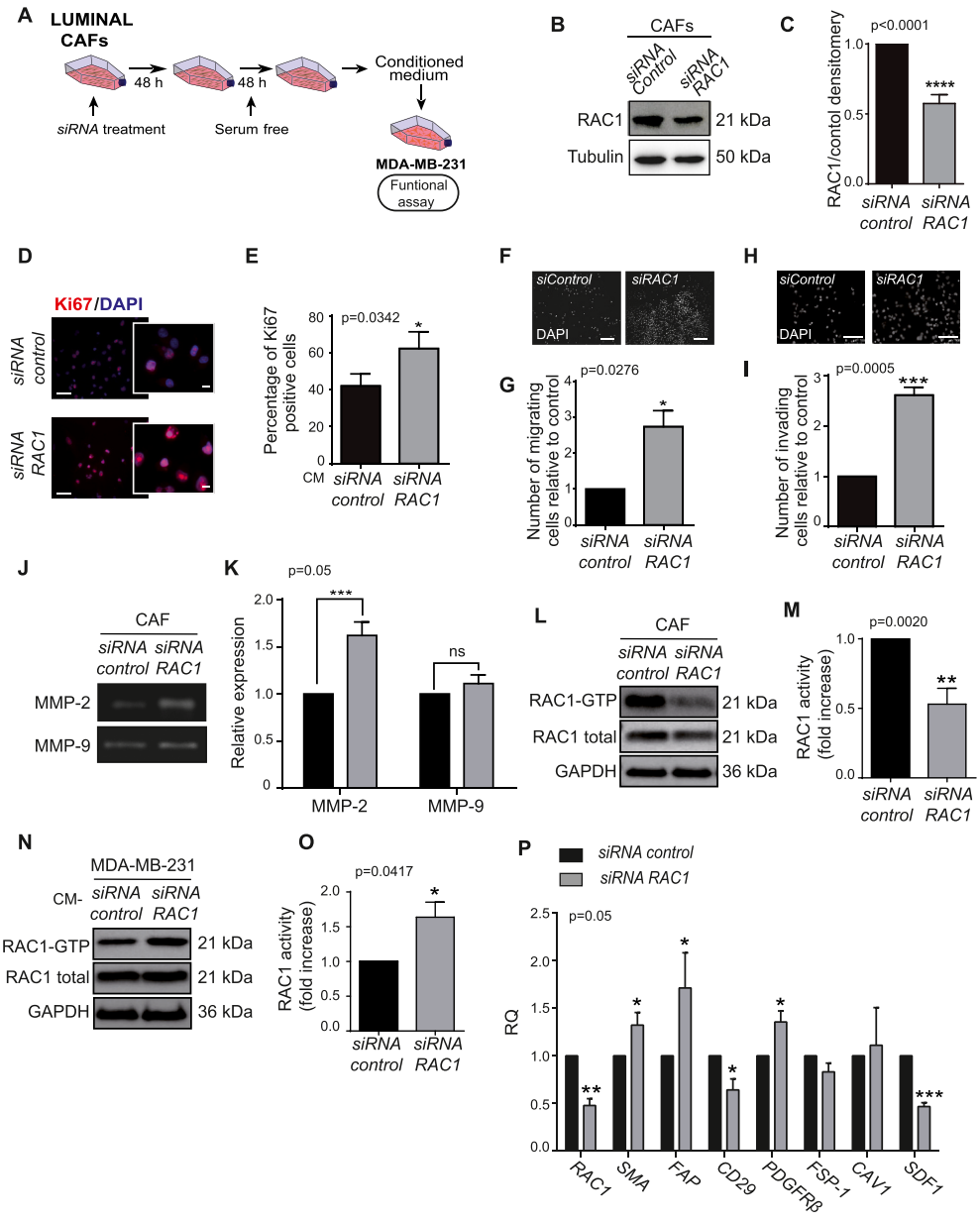

Fig. 4. The genetic depletion of RAC1 is enough to induce the pro-tumorigenic activity of CAFs. (A) Schematic representation of the experimental design where CAFs are treated with a pool of siRNA specific to *RAC1* for 96 h. (B) RAC1 protein in control and RAC1-depleted CAFs analysed in immunoblots probed for RAC1. (C) Densitometry of RAC1 from B from at least three different experiments and determined by scanning densitometry (Mann-Whitney test) (D) Representative image of immunofluorescent evaluation of Ki-67 expression in MDA-MB-231 tumour cells and (E) the percentage of Ki-67-positive cells ($\chi 2$ test) (F) Representative images of MDA-MB-231 migrating cells stained with DAPI. (G) Migrating cells were determined in Boyden chambers as the number of MDA-MB-231 cells treated with CM from CAF-depleted cells that had migrated relative to the CM from control cells (*t*-test) (H) Representative images of cell invasion stained with DAPI. (I) MDA-MB-231 invasion was determined in a matrigel invading assay as the number of invading cells when treated with CM from *RAC1*-depleted CAFs relative to the CM from control cells (*t*-test). (J) Representative zymogram gels corresponding to the degradation bands of MMP-9 and MMP-2. (K) Band quantification from gelatin zymography in J as determined by scanning densitometry (2way ANOVA test; Sidak's post-hoc test). (L) *RAC1* depletion in CAFs reduces the overall RAC1 activity. (M) Quantification of the relative normalized amounts of RAC–GTP in L determined by scanning densitometry (*t*-test). (N) MDA-MB-231 cells treated with CM from L for 24 h and RAC1 activation was assessed in immunoblots. (O) Quantification of the relative normalized amounts of RAC–GTP in N determined by scanning densitometry (*t*-test). (P) Expression of CAF markers in CAFs and CAFs treated with the siRNA RAC1 (*t*-test). Scale bar: 200 μm. The data are the mean ± SEM ($n \geq 3$) and the statistical differences between the groups indicated are denoted as: *P ≤ 0.05; **P ≤ 0.01, ***P ≤ 0.001.

detected an increase in IL-1β production and a more discrete increase in IL-8 in CAFs treated with the Rac inhibitor (Fig. 5B), cytokines that support the growth and progression of carcinomas [6,33–36]. Similar results were obtained when *SDF-1, IL-1β* and *IL-8* mRNA expression was analysed in CAFs by qPCR (Fig. 5C-E). Furthermore, the increase in the expression of the mRNAs encoding these cytokines correlated with that of the IL-1β secreted by CAFs into the CM (Fig. 5F). However, no differences in IL-8 were observed between the CM from CAFs and that from Rac1-inhibited CAFs when analysed by ELISA (Fig. 5G), suggesting that the effects observed were mainly due to IL-1β and not to IL-8. Moreover, genetic depletion of *RAC1* with siRNAs induced IL-1β but not IL-8 secretion by CAFs (Fig. S3B, C). Overall, inhibiting RAC1 activity in CAFs upregulates IL-1β secretion.

To study whether this increase in IL-1β secretion may drive the pro-tumorigenic activity observed after RAC1 inhibition, CAFs were treated with a specific pool of siRNAs to deplete *IL-1β* (Fig. 5H). Genetic depletion of *IL-1β* reduced the secretion of this cytokine into the CM (Fig. 5I) and counteracted the increase in RAC1 activity of MDA-MB-231 cells upon exposure to CM from RAC1-inhibited CAFs (Fig. 5J, K). Similarly, depletion of *IL-1β* in CAFs rescued their influence on the migration and invasion of MDA-MB-231 cells after the inhibition of RAC1 activity (Fig. 5L–O), also by reducing IL-1β secretion (Fig. 5P). As an alternative approach, we targeted IL-1β in the CM using a neutralizing antibody, confirming by ELISA that the antibody neutralized the IL-1β secreted into the medium without affecting the RAC1 activity in CAFs (Fig. 5Q). Thus, we treated CAFs with anti-IL-1β prior to treat cultured BC cells with CM from these CAFs and assess migration. When IL-1β was inhibited in the CM from RAC-inhibited CAFs, MDA-MB-231 migration was no longer observed (Fig. 5R, S), presumably due to the failure to stimulate RAC1 activation in this BC cell line (Fig. 5T, U).

In addition to the activity of RAC1 in the cytosol and at the plasma membrane, RAC1 also appears to translocate to the nucleus to control cell cycle progression and the transcription of some genes [37–39]. Given the increased expression of IL-1β upon RAC1 inactivation, we wondered whether activated RAC1 was being translocated to the nucleus to repress somehow IL-1β transcription in CAFs. Fractionation assays showed that inhibiting RAC1 activity reduced the nuclear translocation of RAC1, supporting this hypothesis (Fig. S3D).

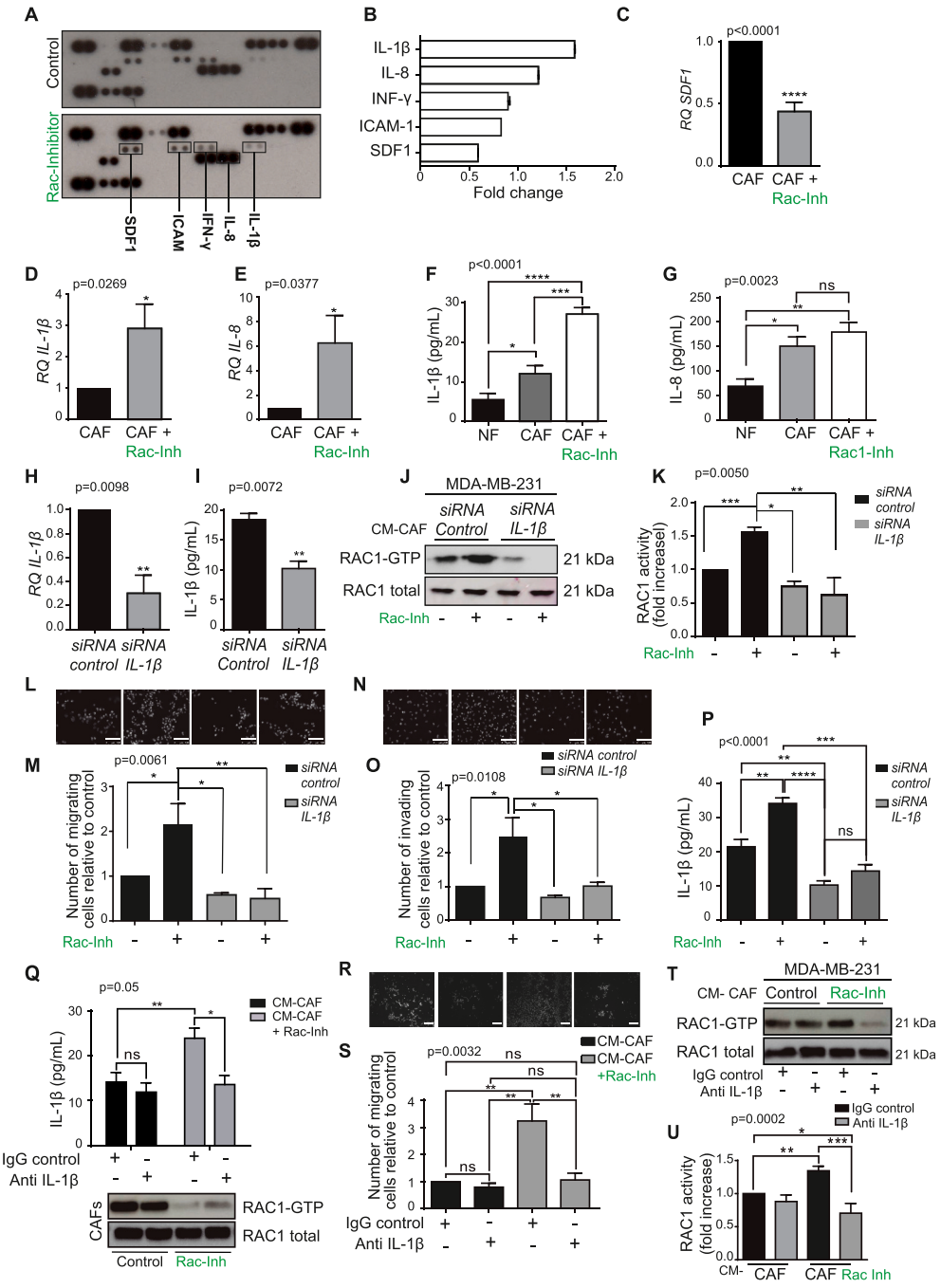

Fig. 5. Inhibition of RAC1 activity alters cytokine production by luminal CAFs. (A) The CM from CAFs and RAC1-inhibited CAFs was analysed using a human cytokine array. (B) ImageJ software was used to quantify the cytokine array shown in A, expressing the fold-change relative to the control CAFs. (C–E) Relative cytokine mRNA expression identified in A and as determined by RT-qPCR from at least 3 independent experiments of the cytokines *SDF-1* (C), *IL-1β* (D) and *IL-8* (E). RQ, relative quantification normalized to the control (*t*-test). (F) The levels of IL-1β and (G) IL-8 in the CM collected from the fibroblasts indicated were measured using a Human Quantikine ELISA kit (ANOVA test; Tukey's post-hoc test). (H) Expression of IL-1β in depleted CAFs was determined by qPCR and (I) IL-1β secretion by ELISA 72 h siRNA post-transfection (*t*-test). RQ, relative quantification normalized to the control. (J) Representative Western blot of RAC1 activity in the MDA-MB-231 BC cell line stimulated with CM from control or *IL-1β*-depleted CAFs in the presence or absence of the Rac-inhibitor. (K) Quantification of the normalized relative amounts of RAC–GTP in J determined by scanning densitometry (2way ANOVA test; Tukey's post-hoc test). (L) Representative images of MDA-MB-231 migrating cells stained with DAPI. (M) MDA-MB-231 migration was determined in Boyden chambers, with the migrating cells determined as the number of MDA-MB-231 cells treated with CM from *IL-1β*-depleted CAFs that had migrated relative to those exposed to CM from control-treated cells (ANOVA test; Tukey's post-hoc test). (N) Representative images of cell invasion stained with DAPI. (O) MDA-MB-231 invading cells were determined as the number of MDA-MB-231 cells treated with CM from *IL-1β*-depleted CAFs relative to those exposed to CM from control cells (ANOVA test; Tukey's post-hoc test). (P) Levels of IL-1β secreted to the CM by siRNA IL-1β depleted CAFs analysed by ELISA (ANOVA test; Tukey's post-hoc test). (Q) IL-1β in CM measured by ELISA after inhibition with IL-1β neutralizing antibody. CAFs treated with Rac-inhibitor have reduced RAC activity (lower panel) and treatment with the neutralizing antibody against IL-1β (40 ng/mL) for 24 h reduced the levels of IL-1β (2way ANOVA test; Sidak's post-hoc test). (R) The CM from Q was used to analyse MDA-MB-231 migration. Representative images of MDA-MB-231 migrating cells stained with DAPI. (S) Number of migrating cells relative to the IgG control in the absence of the Rac-inhibitor (ANOVA test; Tukey's post-hoc test). (T) The CM from Q was used to stimulate MDA-MB-231 cells and RAC1 activity was measured. (U) Quantification of the normalized relative amounts of RAC–GTP in T determined by scanning densitometry (2way ANOVA test; Tukey's post-hoc test). Scale bar: 100–200 μm. The data are the mean ± SEM (n ≥ 3) and the statistical differences between the groups indicated are denoted as: *P ≤ 0.05, **P ≤ 0.01, ***P ≤ 0.001 and ****P ≤ 0.0001.

These results suggest that inhibiting RAC1 activity in CAFs promotes the pro-tumorigenic activity of BC cells by enhancing IL-1β secretion.

3.6. *The pro-tumorigenic activity of CAFs requires intact IL-1β signalling in breast cancer cells*

We found that IL-1β was responsible for the pro-tumorigenic activity of CAFs and thus, we analysed the expression and secretion of IL-1β in the CAFs obtained from different molecular BC subtypes. CAFs

expressed and secreted higher levels of this cytokine (Fig. 6A and B and Fig. S3E), and inhibiting RAC1 activity in luminal CAFs produced similar levels of IL-1β as the TNBC CAFs (Fig. 6C, D). Moreover, the expression of GFP–RAC1V12 in TNBC CAFs reduced the secretion of IL-1B (Fig. S3F).

This data was consistent with the previous results showing that the inhibition of RAC1 activity in luminal CAFs induced a shift towards TNBC-like CAFs (Fig. 3).

We wondered if the CM from RAC1-inhibited CAFs promoted similar effects on migration to those observed in MDA-MB-231 cells by analysing the migration of BC cells of different molecular subtypes, such as Luminal (MCF-7) and Luminal-HER2+ (BT-474) cells. As expected, the CM from CAFs induced the migration of both cell lines but unexpectedly, the CM of RAC1-inhibited CAFs reduced the migratory capacity of these BC cell lines (Fig. 6E-F for MCF-7 and G for BT-474). This reduction was due to a defect in RAC1 activation in both MCF-7 (Fig. 6H, I) and BT-474 cells (Fig. 6J and K).

We wondered why the increase in IL-1β observed after RAC1 inhibition in CAFs did not affect the tumorigenic capacity of MCF-7 and BT-474 cells. Thus, we assayed IL-1β signalling by evaluating the expression of the IL-1β receptor (IL-1R) and IL-1 receptor antagonist (IL-1RA) by qPCR in the three BC cell lines. As seen previously, IL-1R expression was detected in the BT-474 but not the MCF-7 cells (Fig. 6L and reference [40]). However, we detected stronger IL-1RA expression in the BT-474 cells than in the other two cell lines (Fig. 6M and reference [40]). Moreover, we analysed the activation of the IL-1β effector NF-kB (p65) in response to inhibition of RAC1 in Western blots and we found that it was activated in MDA-MB-231 cells, yet not in MCF-7 or BT-474 cells (Fig. S4A). Thus, the increase in IL-1β secretion in response to RAC1 inhibition cannot activate IL-1β signalling in the luminal and luminal-HER2+ BC cell lines. However, these results do not explain why the inhibition of RAC1 activity in CAFs impaired migration and the activation of RAC1 in luminal and HER2+ BC cell lines. As mentioned above, RAC1 inhibition in CAFs reduced the secretion of SDF-1 (Fig. 5B, C and Fig. 6N), an important cytokine implicated in breast tumour migration [11,33]. The addition of recombinant SDF-1 to the CM from RAC-inhibited CAFs was sufficient to rescue tumour cell migration in MCF-7 and BT-474 cells (Fig. 6O, P). However, the enhanced migration of these cells when exposed to SDF-1 was not correlated with activation of the RAC1 GTPase (Figs. S4B–E).

Together, these results suggest that the enhanced pro-tumorigenic activity of CAFs with inhibited RAC1 activity toward BC cells is dependent on IL-1β signalling. To confirm these results, we studied another luminal BC cell line with intact IL-1β signalling, T-47D cells [44]. First, we confirmed that T-47D cells expressed IL-1R by qPCR and that they did not express IL-1RA (Fig. 6Q), such that they can activate the IL-1β effector NFKB (p65) (Fig. S4A). These cells were then treated with CM from luminal CAFs exposed to the Rac inhibitor, which enhanced the migratory capacity of T-47D cells, similar to that obtained with TNBC CAFs (Fig. 6R, S). However, although the CM from CAFs induces RAC1 activity in T-47D cells, the enhanced migration of these cells when exposed to CM from Rac-inhibited Luminal CAFs was not correlated with activation of the RAC1 GTPase in this BC cell line (Fig. 6T, U).

Therefore, the use of RAC1 as a therapeutic target should be considered for breast tumours that cannot transduce IL-1β signals to achieve a full anti-cancer response.

3.7. *Inhibiting RAC1 activity in CAFs promotes tumour proliferation and metastasis in vivo through IL-1β*

To investigate the relevance of our findings *in vivo*, we inoculated the chorioallantoic membrane (CAM) of day 11 chicken embryos with MDA-MB-231 cells expressing GFP in the presence of CAFs or CAFs pre-treated with the Rac inhibitor for 24 h, which were simultaneously treated with either an anti-IL-1β (100 ng/mL) or control isotypic antibody (Fig. 7A). The CAM model system has certain advantages over mice models and for instance, we were able to check that RAC1 inhibition was stable for at least 3 days (Fig. S5A). Thus, we could perform *in vivo* studies with reduced RAC1 activity during the process of tumour initiation and dissemination. In line with the *in vitro* observations, the tumours derived from the co-inoculation of RAC1-inhibited CAFs and MDA-MB-231 cells were larger and heavier than those developed in the other conditions (Fig. 7B, C). Furthermore, using a neutralizing antibody against IL-1β to block the signalling mediated by this interleukin dramatically reduced the rate of tumour growth, while the control antibody had no such effect (Fig. 7B, C).

Recently, PCR-mediated amplification of human specific-Alu sequences has been used for the semi-quantitative detection of disseminated tumour cells in different organs of the chicken embryo [41,42]. Thus, we measure the presence of human Alu sequences in chicken lung tissue to detect metastasis. An increase in relative metastasis was detected when BC cells were co-cultured with CAFs treated with the Rac inhibitor, interestingly, treating these cells with the neutralizing antibody against IL-1β reversed this metastatic phenotype (Fig. 7D, E).

To corroborate the implication of the RAC1 GTPase in tumour development, we investigated whether blocking IL-1β signalling affected the activation of RAC1 GTPase in MDA-MB-231 cell-derived tumours and tumour cell dissemination. The increase in RAC1 activation observed in response to RAC1-inhibited CAFs was abolished in the presence of the neutralizing IL-1β antibody (Fig. 7F, G). Furthermore, the aberrant RAC1 tumour activation affected the activation of the downstream AKT and ERK signalling pathways (Fig. 7H-J), both of them activated in an anomalous manner in cancer [43]. As observed *in vitro* (Fig. 2I), Cyclin D1 expression was enhanced in tumours when RAC1 was inactivated in CAFs (Fig. 7H and K). Furthermore, the co-inoculation of RAC1-inhibited Luminal CAFs and the luminal T-47D BC cell line generated larger and heavier tumours than those that developed in the presence of CAFs (Fig. 7L and Figs. S5B and C).

We have shown that inhibiting RAC1 activity in luminal CAFs promotes the pro-tumourigenic activity of CAFs. Thus, we treated both stromal and tumour cells in this way to assess the therapeutic possibilities of RAC1 inhibition. MDA-MB-231 BC cells were co-cultured in the presence or absence of CAFs and treated with the Rac1 inhibitor at a concentration that reduced RAC1 activity in MDA-MB-231 BC cells (Fig. S5D). The treatment of MDA-MB-231 cells with the Rac inhibitor reduced the growth of tumours generated only with MDA-MB-231 cells, whereas pretreatment of CAFs with the Rac inhibitor led to the generation of larger tumours when these cells were inoculated together with MDA-MB-231 cells (Fig. 7M and Fig. S5E, F). Interestingly, when tumours generated with co-cultured MDA-MB-321 and CAFs were treated with the Rac inhibitor they grew significantly more than the untreated tumours. Importantly, blockade of IL-1β signalling abrogated the effect of RAC1 inhibition in the above models (Fig. 7M, N), provoking less proliferative and less metastatic tumours, as observed *in vitro* (Fig. S5G-I).

All these results support the idea that inhibiting RAC1 activity in CAFs promotes tumour proliferation and metastasis *in vivo* through IL-1β, making RAC1-GTP inhibition a potential therapeutic strategy for breast tumours with defects in IL-1β signalling. Moreover, combining the use of a Rac inhibitor with IL-1β inactivation could be the best therapeutic option in breast cancer (Fig. 7O).

4. Discussion

Breast cancer represents the leading cause of neoplastic disease in women, with an annual incidence of more than two million new cases [1]. The diagnosis and treatment of BC is defined by molecular and histological parameters, yet there is evidence that a complex TME has the potential to influence its evolution and therapeutic responses [9,23,44]. Fibroblasts represent a major component of the TME and there is a large amount of data demonstrating their capacity to promote cancer

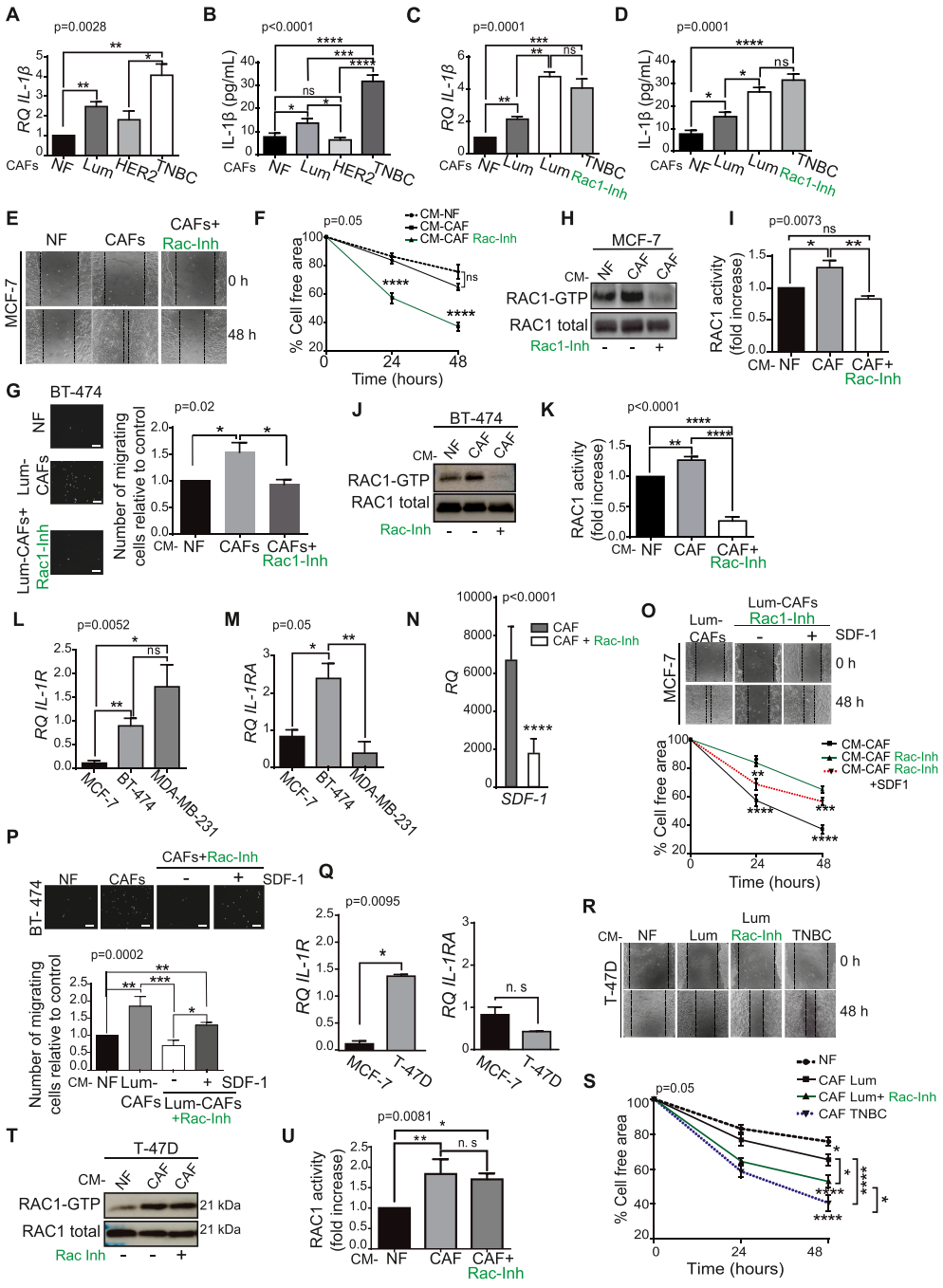

Fig. 6. The pro-tumorigenic activity of CAFs requires intact IL-1β signalling in breast cancer cells. (A) Expression of *IL-1β* in the CAFs indicated, assessed by RT-qPCR in at least 3 different experiments (ANOVA test; Tukey's post-hoc test). RQ, relative quantification normalized to the control (B) The IL-1β in the CM collected from the fibroblasts indicated was measured using a Human Quantikine ELISA kit (ANOVA test; Tukey's post-hoc test). (C) Expression of *IL-1β* in NFs, luminal, Luminal Rac1-inhibited and TNBC CAFs assessed by RT-qPCR in at least 3 different experiments (ANOVA test; Tukey's post-hoc test). RQ, relative quantification normalized to the control (D) IL-1β in the CM collected from the fibroblasts indicated were measured using a Human Quantikine ELISA kit (ANOVA test; Tukey's post-hoc test). (E) Representative images of MCF-7 migrating cells. (F) Migrating cells were determined in wound assay as the gap closure of MCF-7 cells treated with the indicated CM (2way ANOVA Sidak's multiple comparisons test). (G) Representative images of BT-474 migrating cells stained with DAPI and cell migration was assayed in Boyden chambers as the number of BT-474 cells treated with CM from RAC1-inhibited CAFs that had migrated relative to those exposed to CM from control cells (ANOVA test; Tukey's post-hoc test). (H) Representative Western blot of RAC1 activity in the MCF-7 BC cell line stimulated with CM from control or RAC1 inhibited CAFs. (I) Quantification of the relative normalized amounts of RAC–GTP in G determined by scanning densitometry (ANOVA test; Tukey's post-hoc test). (J) Representative Western blot of RAC1 activity in the BT-474 BC cell line stimulated with CM from control or RAC1 inhibited CAFs. (K) Quantification of the relative normalized amounts of RAC–GTP in J determined by scanning densitometry (ANOVA test; Tukey's post-hoc test). (L, M) Analysis of *IL-1R* (L) and *IL*-1RA (M) expression by RT-qPCR from at least 3 different experiments (ANOVA test; Tukey's post-hoc test). (N) Relative SDF-1 mRNA expression determined by RT-qPCR from at least 3 independent experiments (*t*-test). (O) Representative images of MCF-7 migrating cells in the presence of SDF-1 (50 ng/ml). Migrating cells were determined in wound assay as the gap closure of MCF-7 cells treated with CM from RAC1-inhibited CAFs in the presence of SDF-1 (Sidak's multiple comparisons test). The graph combines the controls from F plus the SDF-1 condition. (P) Representative images of BT-474 migrating cells stained with DAPI in the presence of SDF-1 (50 ng/ml). Cell migration was assayed in Boyden chambers as the number of BT-474 cells, treated with CM from RAC1-inhibited CAFs in the presence of recombinant SDF-1, that had migrated relative to those exposed to CM from control cells (ANOVA test; Tukey's post-hoc test). (Q) Analysis of the *IL-1R* and *IL*-1RA expression in T-47D cells by RT-qPCR from at least 3 different experiments (*t*-test). RQ, relative quantification normalized to the control (R) Representative images of T-47D migrating cells. (S) Migrating cells were assessed in wound assay as the gap closure of T-47D cells treated with the CM indicated (Sidak's multiple comparisons test). (T) Representative Western blot of RAC1 activity in the T-47D BC cell line stimulated with CM from control or RAC1-inhibited CAFs. (U) Quantification of the relative normalized amounts of RAC–GTP in T determined by scanning densitometry (ANOVA test; Tukey's post-hoc test). RQ, relative quantification. Scale bar: 100 μm. The data are the mean ± SEM (n ≥ 3) and the statistical differences between the groups indicated are denoted as: *P ≤ 0.05, **P ≤ 0.01, ***P ≤ 0.001 and ****P ≤ 0.0001.

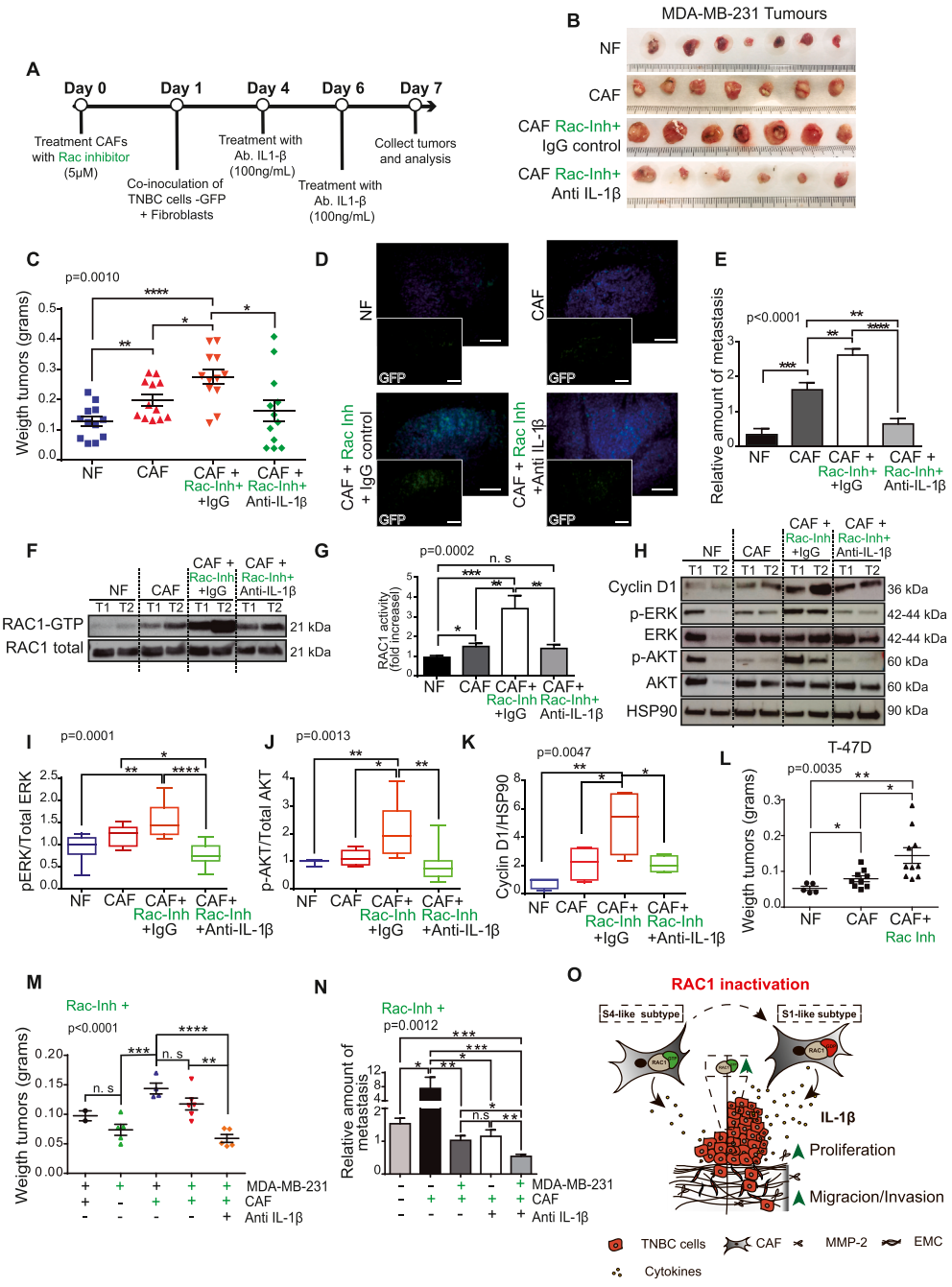

Fig. 7. Inhibition of RAC1 activity in CAFs promotes tumour proliferation and metastasis *in vivo* through IL-1β. (A) Schematic representation of the experimental design. One day before the *in vivo* experiment, CAFs were treated with the Rac-inhibitor for 24 h and the GFP positive MDA-MB-231 cells were then used to generate tumours in chicken embryos over 7 days. Two treatments with the neutralizing IL-1β antibody (100 ng/mL) or isotopic control were delivered. (B) Representative images of tumours obtained from xenografts co-inoculated with fibroblasts. (C) Tumour weight 7 days after co-inoculation of the chorioallantoic membrane (CAM) (ANOVA test; Tukey's post-hoc test). (D) GFP detection in tumours treated with the RAC-inhibitor and neutralizing IL-1β or control antibodies by immunofluorescence. (E) Quantitative detection of MDA-MB-231 cells in the embryonic lungs assays using the Alu sequences (ANOVA test; Tukey's post-hoc test). (F) Representative Immunoblot of RAC1 activity in tumours from the xenograft. T1 and T2 are tumours derived from the same condition. (G) The RAC1-GTP bands were quantified and the normalized intensities were calculated relative to the controls (n = 8 tumours per group) (ANOVA test; Tukey's post-hoc test). (H) Representative Immunoblot of AKT, ERK activity and Cyclin D1 expression in tumours from the xenograft. (I–K) Proteins of pERK/ERK (I), pAKT/AKT (J), Cyclin D1 (K) from H were quantified and the normalized intensities were calculated relative to the controls (n = 8 tumours per group) (ANOVA test; Tukey's post-hoc test). (L) Tumour weight 7 days after co-inoculation of the chorioallantoic membrane (CAM) with T-47D cells and luminal CAFs treated with the Rac inhibitor (ANOVA test; Tukey's post-hoc test). (M) Tumour weight 7 days after co-inoculation with the treated cells of the CAM indicated. The cells were treated with the Rac inhibitor or the IL-1β neutralizing antibody 4 and 6 days after the inoculation (ANOVA test; Tukey's post-hoc test) (N) Quantitative detection of MDA-MB-231 cells in the embryonic lung assays using the Alu sequences (ANOVA test; Tukey's post-hoc test). (O) Working model of the mechanisms by which RAC1 can regulate the BC microenvironment. Scale bar: 200 μm. The data are the mean ± SEM (n ≥ 3) and the statistical differences between the groups indicated are denoted as: as *P ≤ 0.05, **P ≤ 0.01, ***P ≤ 0.001 and ****P ≤ 0.0001.

through paracrine effects, escorting tumour cells through all the steps of carcinogenesis [33,45,46]. Here we illustrate some of the complex interactions in the tumour-host microenvironment.

RAC1 is a molecular switch that fluctuates between the inactive GDP-bound (RAC1-GDP) and the active GTP-bound form (RAC1-GTP), and it is involved in a wide range of functions, mainly in the control of cytoskeletal reorganization associated with cell motility in normal and malignant cells like breast carcinoma cells [47]. In a cancer context, the enhanced activation of this protein has been implicated in metastasis and invasiveness, and it is considered a poor-prognostic factor associated with therapeutic resistance [48,49]. Different studies support the role of RAC1 activation in promoting the migration and invasion of epithelial tumour cells. Thus, inactivation of RAC1 in the epithelial compartment is considered a good strategy to inhibit tumour dissemination. However, the implication of RAC1 in the TME has yet to be fully analysed.

Using a pharmacological inhibitor of RAC1 activity (EHop-016) we found that the inactivation of RAC1 in CAFs stimulates tumour cell migration and invasion by BC cells in which IL-1β signalling remains intact, such as the TNBC MDA-MB-231 and luminal T-47D cell lines. Among the cytokines identified, IL-1β is the only cytokine that displays enhanced transcription and secretion into the medium. There is

considerable evidence that IL-1β is secreted by CAFs [34,36,50] and it has long been proposed as an important cytokine for metastasis, both in breast and other cancers [35,51,52] in which RAC1 may be activated [53,54]. Nonetheless, the direct regulation of IL-1β by RAC1 has not yet be demonstrated. There are reports suggesting that IL-1β secretion is mediated by active RAC1 (RAC1-GTP bound) [55,56]. However, here we report that CAFs with the inactive form of RAC1 (RAC1-GDP bound) are responsible for the upregulation of this cytokine and the fractionation experiments carried out suggest that RAC1 may repress IL-1β expression. Moreover, constitutive activation of RAC1 in TNBC CAF cells reduces IL-1β secretion, further supporting this idea.

The cytokine IL-1β can upregulate a variety of processes that contribute to angiogenesis, or tumour growth and BC progression, and it is considered a strong and causative pro-malignancy factor whose expression is associated with an advanced disease [35,57,58]. We found that the pro-tumorigenic effect of CAFs was enhanced by RAC1 inactivation and that this depended on IL-1β, both *in vivo* and *in vitro*. Indeed, targeting IL-1β has been considered a strategy to block breast tumour development and that of other types of cancer [51,59,60]. Surprisingly, the pro-tumorigenic effect of RAC1-inhibited CAFs was not observed in luminal and HER2+ BC molecular subtypes where IL-1β signalling pathway was not functional, either because they do not express the receptor for IL-1β or because they express high levels of the IL-1β antagonist. Under these circumstances, the inhibition of RAC1 activity in CAFs did reduce the migratory capacity of these BC cell lines due to a reduction in SDF-1.

These results highlight the relevance of the fine regulation and balance of all tumour effectors in both the epithelial and stromal compartments, where RAC1 seems to fulfil a crucial role. As a result, inhibiting RAC1 activity in CAFs alters their secretory phenotype, which may produce either pro-tumorigenic or tumour-suppressor effects depending on the molecular context. On the one hand, RAC1 inhibition in CAFs not only promotes the expression of IL-1β but also its secretion, which induces RAC1 activation and is accompanied by the proliferation, migration and invasion of TNBC and luminal T-47D cells. However, it should not be ignored that RAC1-inhibited CAFs produce less SDF-1, INF-γ and ICAM-1, all of which are important in the tumorigenic process [61]. Indeed, BC associated CAFs secrete SDF-1 that stimulates tumour growth and invasion of breast carcinoma [11,33].

In a cellular context where IL-1β is not impeded (IL-1R is available and IL-1AR is absent), this cytokine counteracts the lack of protumourigenic signals like SDF-1, and it drives a proliferative and invasive response in cancer cells, as observed in TNBC MDA-MB-231 cells. Indeed, there is evidence that HER2-negative BC has an IL-1β transcriptional signature and that the levels of IL-1β are correlated with poor survival [61]. By contrast, when IL-1β signalling is impaired, the lack of tumoural factors takes the lead and carcinoma cells adopt a less migratory phenotype, with less RAC1 activation. This is the case of the luminal MCF-7 and HER2+ BT-474 cells studied here, suggesting that RAC1 inhibition might be a good strategy to block metastasis in this type of breast carcinoma, with a defect in IL-1β signalling.

Our study not only adds further weight to the secretory changes as a consequence of RAC1 inactivation in CAFs but also, for the first time we demonstrated that the activity of a small GTPase drives changes in CAF expression profiles. CAFs are known to be heterogeneous in breast tumours but the nature of this heterogeneity and its link with CAF activities is still far from clear [13,17]. We hypothesized that RAC1 inactivation drives changes in the CAFs promoting functions similar to CAF-S1-like, such as a pro-inflammatory phenotype and IL-1β secretion [13]. Indeed, a recent report showed that IL-1 signalling may shape CAF heterogeneity in Pancreatic Ductal Adenocarcinoma (PDA), promoting differentiation at pro-inflammatory CAF subset [62]. Moreover, we demonstrate that inhibiting RAC1 activity and inactivating IL-1β is the best therapeutic option in BC due to dual role of RAC1 in tumour development. On the one hand, RAC1 promotes tumorigenic properties in the epithelial compartment but on the other hand, RAC1 activity inhibits the pro-tumorigenic activity of the stromal compartment. Thus, inactivation of RAC1 and IL-1β may a good strategy to limit BC malignancy.

Overall, the data presented here enhance our understanding of the mechanisms by which RAC1 can regulate the BC microenvironment. Specifically, we found that inhibiting RAC1 in CAFs increases aggressiveness by upregulating IL-1β. These findings shed light on the complexity of the interplay in the tumour cell-microenvironment and they should be taken into consideration in the study of therapeutic strategies aimed at targeting RAC1, especially in the case of breast tumours with intact IL-1β signalling.

Financial Support

A.M-L is supported by a Consejo Nacional de Ciencia y Tecnología (CONACYT) Pre-doctoral Training Grant. A.G.-C. is the recipient of a FPU grant from the Spanish Ministry of Science, Innovation and University. P.B-D work was supported by a MINECO/FEDER research grant (PID2019-104991RB-I00). S.C.-L. was the recipient of a Ramón y Cajal research contract from the Spanish Ministry of Economy and Competitiveness. The work carried out by the group of S.C-L was supported by a MINECO/FEDER research grant (SAF2015-64499-R; RTI2018-094130-B-100).

Availability of data and materials

The data sets obtained and/or analysed in the current study are available from the corresponding author upon reasonable request.

Author contributions

A.M.L carried out all the experiments, apart from the CAM xenografts that were performed with the help of P.B. A.G.C helped with the Alu sequencing, MCF7 GTPase assays and some *in vitro* experiments with RAC1-inhibited MDA-MB-231 cells. P.B provided the different CAF subtypes, apart from the luminal CAFs that was provided by A.O. S.C.L. provided team leadership, project management and wrote the manuscript.

CRediT authorship contribution statement

Angélica Martínez-López: Conceptualization, Methodology, Formal analysis, Investigation, Writing – review & editing. **Ana García-Casas:** Investigation. **Paloma Bragado:** Investigation. **Akira Orimo:** Methodology. **Eduardo Castañeda-Saucedo:** Supervision. **Sonia Castillo-Lluva:** Conceptualization, Formal analysis, Investigation, Writing – review & editing, Supervision, Project administration, Funding acquisition.

Acknowledgments

We thank Nélida Salvador and Alberto Meca for their technical assistance. We thank Cristina Baquero Mayo for her help in obtaining the paraffin blocks.

Appendix A. Supplementary data

Supplementary data to this article can be found online at https://doi.org/10.1016/j.canlet.2021.08.014.

Declaration of competing interest

The authors declare that they have no known competing financial interests or personal relationships that could have appeared to influence the work reported in this paper.

References

[1] H. Sung, J. Ferlay, R.L. Siegel, M. Laversanne, I. Soerjomataram, A. Jemal, F. Bray, Global cancer statistics 2020: GLOBOCAN estimates of incidence and mortality worldwide for 36 cancers in 185 countries, CA Cancer J Clin, 2021.

[2] C.M. Perou, T. Sorlie, M.B. Eisen, M. van de Rijn, S.S. Jeffrey, C.A. Rees, J. R. Pollack, D.T. Ross, H. Johnsen, L.A. Akslen, O. Fluge, A. Pergamenschikov, C. Williams, S.X. Zhu, P.E. Lonning, A.L. Borresen-Dale, P.O. Brown, D. Botstein, Molecular portraits of human breast tumours, Nature 406 (2000) 747–752.

[3] A. Schnelzer, D. Prechtel, U. Knaus, K. Dehne, M. Gerhard, H. Graeff, N. Harbeck, M. Schmitt, E. Lengyel, Rac1 in human breast cancer: overexpression, mutation analysis, and characterization of a new isoform, Rac1b, Oncogene 19 (2000) 3013–3020.

[4] A.L. Hein, C.M. Post, Y.M. Sheinin, I. Lakshmanan, A. Natarajan, C.A. Enke, S. K. Batra, M.M. Ouellette, Y. Yan, RAC1 GTPase promotes the survival of breast cancer cells in response to hyper-fractionated radiation treatment, Oncogene 35 (2016) 6319–6329.

[5] R.G. Hodge, A.J. Ridley, Regulating Rho GTPases and their regulators, Nat. Rev. Mol. Cell Biol. 17 (2016) 496–510.

[6] Y. Mezawa, A. Orimo, The roles of tumor- and metastasis-promoting carcinoma-associated fibroblasts in human carcinomas, Cell Tissue Res. 365 (2016) 675–689.

[7] K.G.K. Deepak, R. Vempati, G.P. Nagaraju, V.R. Dasari, S. Nagini, D.N. Rao, R. R. Malla, Tumor microenvironment: challenges and opportunities in targeting metastasis of triple negative breast cancer, Pharmacol. Res. 153 (2020) 104683.

[8] R.E. Coleman, W. Gregory, H. Marshall, C. Wilson, I. Holen, The metastatic microenvironment of breast cancer: clinical implications, Breast 22 (Suppl 2) (2013) S50–S56.

[9] H.M. Brechbuhl, A.S. Barrett, E. Kopin, J.C. Hagen, A.L. Han, A.E. Gillen, J. Finlay-Schultz, D.M. Cittelly, P. Owens, K.B. Horwitz, C.A. Sartorius, K. Hansen, P. Kabos, Fibroblast subtypes define a metastatic matrisome in breast cancer, JCI Insight (2020) 5.

[10] E. Pure, R. Blomberg, Pro-tumorigenic roles of fibroblast activation protein in cancer: back to the basics, Oncogene 37 (2018) 4343–4357.

[11] A. Blanco-Gomez, L. Hontecillas-Prieto, R. Corchado-Cobos, N. Garcia-Sancha, N. Salvador, A. Castellanos-Martin, M.D.M. Saez-Freire, M. Mendiburu-Elicabe, D. Alonso-Lopez, J. De Las Rivas, M. Lorente, A. Garcia-Casas, S. Del Carmen, M.D. M. Abad-Hernandez, J.J. Cruz-Hernandez, C.A. Rodriguez-Sanchez, J. Claros-Ampuero, B. Garcia-Cenador, J. Garcia-Criado, A. Orimo, T. Gridley, J. Perez-Losada, S. Castillo-Lluva, Stromal SNAI2 is required for ERBB2 breast cancer progression, Canc. Res. 80 (2020) 5216–5230.

[12] A. Glentis, P. Oertle, P. Mariani, A. Chikina, F. El Marjou, Y. Attieh, F. Zaccarini, M. Lae, D. Loew, F. Dingli, P. Sirven, M. Schoumacher, B.G. Gurchenkov, M. Plodinec, D.M. Vignjevic, Author Correction: cancer-associated fibroblasts induce metalloprotease-independent cancer cell invasion of the basement membrane, Nat. Commun. 9 (2018) 1036.

[13] A. Costa, Y. Kieffer, A. Scholer-Dahirel, F. Pelon, B. Bourachot, M. Cardon, P. Sirven, I. Magagna, L. Fuhrmann, C. Bernard, C. Bonneau, M. Kondratova, I. Kuperstein, A. Zinovyev, A.M. Givel, M.C. Parrini, V. Soumelis, A. Vincent-Salomon, F. Mechta-Grigoriou, Fibroblast heterogeneity and immunosuppressive environment in human breast cancer, Canc. Cell 33 (2018) 463–479 e410.

[14] M. Kurashige, M. Kohara, K. Ohshima, S. Tahara, Y. Hori, S. Nojima, N. Wada, J. I. Ikeda, K. Miyamura, M. Ito, E. Morii, Origin of cancer-associated fibroblasts and tumor-associated macrophages in humans after sex-mismatched bone marrow transplantation, Commun Biol 1 (2018) 131.

[15] Y. Kieffer, H.R. Hocine, G. Gentric, F. Pelon, C. Bernard, B. Bourachot, S. Lameiras, L. Albergante, C. Bonneau, A. Guyard, K. Tarte, A. Zinovyev, S. Baulande, G. Zalcman, A. Vincent-Salomon, F. Mechta-Grigoriou, Single-cell analysis reveals fibroblast clusters linked to immunotherapy resistance in cancer, Canc. Discov. 10 (2020) 1330–1351.

[16] C. Bonneau, A. Elies, Y. Kieffer, B. Bourachot, S. Ladoire, F. Pelon, D. Hequet, J. M. Guinebretiere, C. Blanchet, A. Vincent-Salomon, R. Rouzier, F. Mechta-Grigoriou, A subset of activated fibroblasts is associated with distant relapse in early luminal breast cancer, Breast Cancer Res. 22 (2020) 76.

[17] F. Pelon, B. Bourachot, Y. Kieffer, I. Magagna, F. Mermet-Meillon, I. Bonnet, A. Costa, A.M. Givel, Y. Attieh, J. Barbazan, C. Bonneau, L. Fuhrmann, S. Descroix, D. Vignjevic, P. Silberzan, M.C. Parrini, A. Vincent-Salomon, F. Mechta-Grigoriou, Cancer-associated fibroblast heterogeneity in axillary lymph nodes drives metastases in breast cancer through complementary mechanisms, Nat. Commun. 11 (2020) 404.

[18] A. Mogilner, K. Keren, The shape of motile cells, Curr. Biol. 19 (2009) R762–R771.

[19] S. Liu, M. Kapoor, A. Leask, Rac1 expression by fibroblasts is required for tissue repair in vivo, Am. J. Pathol. 174 (2009) 1847–1856.

[20] A. Acevedo, C. Gonzalez-Billault, Crosstalk between Rac1-mediated actin regulation and ROS production, Free Radical Biol. Med. 116 (2018) 101–113.

[21] N.A. Mack, H.J. Whalley, S. Castillo-Lluva, A. Malliri, The diverse roles of Rac signaling in tumorigenesis, Cell Cycle 10 (2011) 1571–1581.

[22] Y. Kojima, A. Acar, E.N. Eaton, K.T. Mellody, C. Scheel, I. Ben-Porath, T.T. Onder, Z.C. Wang, A.L. Richardson, R.A. Weinberg, A. Orimo, Autocrine TGF-beta and stromal cell-derived factor-1 (SDF-1) signaling drives the evolution of tumor-promoting mammary stromal myofibroblasts, Proc. Natl. Acad. Sci. U. S. A. 107 (2010) 20009–20014.

[23] P. Fernandez-Nogueira, M. Mancino, G. Fuster, A. Lopez-Plana, P. Jauregui, V. Almendro, E. Enreig, S. Menendez, F. Rojo, A. Noguera-Castells, A. Bill, L. A. Gaither, L. Serrano, L. Recalde-Percaz, N. Moragas, R. Alonso, E. Ametller, A. Rovira, A. Lluch, J. Albanell, P. Gascon, P. Bragado, Tumor-associated fibroblasts promote HER2-targeted therapy resistance through FGFR2 activation, Clin. Canc. Res. 26 (2020) 1432–1448.

[24] S. Castillo-Lluva, M.H. Tatham, R.C. Jones, E.G. Jaffray, R.D. Edmondson, R. T. Hay, A. Malliri, SUMOylation of the GTPase Rac1 is required for optimal cell migration, Nat. Cell Biol. 12 (2010) 1078–1085.

[25] B.L. Montalvo-Ortiz, L. Castillo-Pichardo, E. Hernandez, T. Humphries-Bickley, A. De la Mota-Peynado, L.A. Cubano, C.P. Vlaar, S. Dharmawardhane, Characterization of EHop-016, novel small molecule inhibitor of Rac GTPase, J. Biol. Chem. 287 (2012) 13228–13238.

[26] S. Castillo-Lluva, L. Hontecillas-Prieto, A. Blanco-Gomez, M. Del Mar Saez-Freire, B. Garcia-Cenador, J. Garcia-Criado, M. Perez-Andres, A. Orfao, M. Canamero, J. H. Mao, T. Gridley, A. Castellanos-Martin, J. Perez-Losada, A new role of SNAI2 in postlactational involution of the mammary gland links it to luminal breast cancer development, Oncogene 34 (2015) 4797–4798.

[27] J. Kim, W. Yu, K. Kovalski, L. Ossowski, Requirement for specific proteases in cancer cell intravasation as revealed by a novel semiquantitative PCR-based assay, Cell 94 (1998) 353–362.

[28] A.P. Porter, A. Papaioannou, A. Malliri, Deregulation of Rho GTPases in cancer, Small GTPases 7 (2016) 123–138.

[29] X.J. Ma, S. Dahiya, E. Richardson, M. Erlander, D.C. Sgroi, Gene expression profiling of the tumor microenvironment during breast cancer progression, Breast Cancer Res. 11 (2009) R7.

[30] M.K. Mittal, K. Singh, S. Misra, G. Chaudhuri, SLUG-induced elevation of D1 cyclin in breast cancer cells through the inhibition of its ubiquitination, J. Biol. Chem. 286 (2011) 469–479.

[31] K. Kessenbrock, V. Plaks, Z. Werb, Matrix metalloproteinases: regulators of the tumor microenvironment, Cell 141 (2010) 52–67.

[32] A. Taguchi, K. Kawana, K. Tomio, A. Yamashita, Y. Isobe, K. Nagasaka, K. Koga, T. Inoue, H. Nishida, S. Kojima, K. Adachi, Y. Matsumoto, T. Arimoto, O. Wada-Hiraike, K. Oda, J.X. Kang, H. Arai, M. Arita, Y. Osuga, T. Fujii, Matrix metalloproteinase (MMP)-9 in cancer-associated fibroblasts (CAFs) is suppressed by omega-3 polyunsaturated fatty acids in vitro and in vivo, PloS One 9 (2014), e89605.

[33] A. Orimo, P.B. Gupta, D.C. Sgroi, F. Arenzana-Seisdedos, T. Delaunay, R. Naeem, V. J. Carey, A.L. Richardson, R.A. Weinberg, Stromal fibroblasts present in invasive human breast carcinomas promote tumor growth and angiogenesis through elevated SDF-1/CXCL12 secretion, Cell 121 (2005) 335–348.

[34] J. Zhang, S. Li, Y. Zhao, P. Ma, Y. Cao, C. Liu, X. Zhang, W. Wang, L. Chen, Y. Li, Cancer-associated fibroblasts promote the migration and invasion of gastric cancer cells via activating IL-17a/JAK2/STAT3 signaling, Ann. Transl. Med. 8 (2020) 877.

[35] I. Holen, D.V. Lefley, S.E. Francis, S. Rennicks, S. Bradbury, R.E. Coleman, P. Ottewell, IL-1 drives breast cancer growth and bone metastasis in vivo, Oncotarget 7 (2016) 75571–75584.

[36] S. Chatterjee, V. Bhat, A. Berdnikov, J. Liu, G. Zhang, E. Buchel, J. Safneck, A. J. Marshall, L.C. Murphy, L.M. Postovit, A. Raouf, Paracrine crosstalk between fibroblasts and ER(+) breast cancer cells creates an IL1beta-enriched niche that promotes tumor growth, iScience 19 (2019) 388–401.

[37] D. Michaelson, W. Abidi, D. Guardavaccaro, M. Zhou, I. Ahearn, M. Pagano, M. R. Philips, Rac1 accumulates in the nucleus during the G2 phase of the cell cycle and promotes cell division, J. Cell Biol. 181 (2008) 485–496.

[38] C. Jamieson, C. Lui, M.G. Brocardo, E. Martino-Echarri, B.R. Henderson, Rac1 augments Wnt signaling by stimulating beta-catenin-lymphoid enhancer factor-1 complex assembly independent of beta-catenin nuclear import, J. Cell Sci. 128 (2015) 3933–3946.

[39] I. Navarro-Lerida, T. Pellinen, S.A. Sanchez, M.C. Guadamillas, Y. Wang, T. Mirtti, E. Calvo, M.A. Del Pozo, Rac1 nucleocytoplasmic shuttling drives nuclear shape changes and tumor invasion, Dev. Cell 32 (2015) 318–334.

[40] C.F. Singer, N. Kronsteiner, G. Hudelist, E. Marton, I. Walter, M. Kubista, K. Czerwenka, M. Schreiber, M. Seifert, E. Kubista, Interleukin 1 system and sex steroid receptor expression in human breast cancer: interleukin 1alpha protein secretion is correlated with malignant phenotype, Clin. Canc. Res. 9 (2003) 4877–4883.

[41] M.A. Batzer, P.L. Deininger, Alu repeats and human genomic diversity, Nat. Rev. Genet. 3 (2002) 370–379.

[42] E.H. van der Horst, J.H. Leupold, R. Schubbert, A. Ullrich, H. Allgayer, TaqMan-based quantification of invasive cells in the chick embryo metastasis assay, Biotechniques 37 (2004) 940–942, 944, 946.

[43] K.S. Saini, S. Loi, E. de Azambuja, O. Metzger-Filho, M.L. Saini, M. Ignatiadis, J. E. Dancey, M.J. Piccart-Gebhart, Targeting the PI3K/AKT/mTOR and Raf/MEK/ERK pathways in the treatment of breast cancer, Canc. Treat Rev. 39 (2013) 935–946.

[44] A.E. Place, S. Jin Huh, K. Polyak, The microenvironment in breast cancer progression: biology and implications for treatment, Breast Cancer Res. 13 (2011) 227.

[45] A.M. Hammer, G.M. Sizemore, V.C. Shukla, A. Avendano, S.T. Sizemore, J. J. Chang, R.D. Kladney, M.C. Cuitino, K.A. Thies, Q. Verfurth, A. Chakravarti, L. D. Yee, G. Leone, J.W. Song, S.N. Ghadiali, M.C. Ostrowski, Stromal PDGFR-alpha activation enhances matrix stiffness, impedes mammary ductal development, and accelerates tumor growth, Neoplasia 19 (2017) 496–508.

[46] P. Gascard, T.D. Tlsty, Carcinoma-associated fibroblasts: orchestrating the composition of malignancy, Genes Dev. 30 (2016) 1002–1019.

[47] P. De, J.H. Carlson, T. Jepperson, S. Willis, B. Leyland-Jones, N. Dey, RAC1 GTPase signals Wnt-beta-catenin pathway mediated integrin-directed metastasis-associated tumor cell phenotypes in triple negative breast cancers, Oncotarget 8 (2017) 3072–3103.

[48] M. Yamaguchi, K. Takagi, A. Sato, Y. Miki, M. Miyashita, H. Sasano, T. Suzuki, Rac1 activation in human breast carcinoma as a prognostic factor associated with therapeutic resistance, Breast Cancer 27 (2020) 919–928.
[49] W. Liu, J. Han, S. Shi, Y. Dai, J. He, TUFT1 promotes metastasis and chemoresistance in triple negative breast cancer through the TUFT1/Rab5/Rac1 pathway, Canc. Cell Int. 19 (2019) 242.
[50] D. Zhang, L. Li, H. Jiang, Q. Li, A. Wang-Gillam, J. Yu, R. Head, J. Liu, M. B. Ruzinova, K.H. Lim, Tumor-stroma IL1beta-IRAK4 feedforward circuitry drives tumor fibrosis, chemoresistance, and poor prognosis in pancreatic cancer, Canc. Res. 78 (2018) 1700–1712.
[51] R. Eyre, D.G. Alferez, A. Santiago-Gomez, K. Spence, J.C. McConnell, C. Hart, B. M. Simoes, D. Lefley, C. Tulotta, J. Storer, A. Gurney, N. Clarke, M. Brown, S. J. Howell, A.H. Sims, G. Farnie, P.D. Ottewell, R.B. Clarke, Microenvironmental IL1beta promotes breast cancer metastatic colonisation in the bone via activation of Wnt signalling, Nat. Commun. 10 (2019) 5016.
[52] M.R. Bani, A. Garofalo, E. Scanziani, R. Giavazzi, Effect of interleukin-1-beta on metastasis formation in different tumor systems, J Natl Cancer Inst 83 (1991) 119–123.
[53] M. Windheim, B. Hansen, Interleukin-1-induced activation of the small GTPase Rac1 depends on receptor internalization and regulates gene expression, Cell. Signal. 26 (2014) 49–55.
[54] J. Franco-Barraza, J.E. Valdivia-Silva, H. Zamudio-Meza, A. Castillo, E.A. Garcia-Zepeda, L. Benitez-Bribiesca, I. Meza, Actin cytoskeleton participation in the onset of IL-1beta induction of an invasive mesenchymal-like phenotype in epithelial MCF-7 cells, Arch. Med. Res. 41 (2010) 170–181.
[55] J. Eitel, K. Meixenberger, C. van Laak, C. Orlovski, A. Hocke, B. Schmeck, S. Hippenstiel, P.D. N'Guessan, N. Suttorp, B. Opitz, Rac1 regulates the NLRP3 inflammasome which mediates IL-1beta production in Chlamydophila pneumoniae infected human mononuclear cells, PloS One 7 (2012), e30379.
[56] C.A. Jefferies, L.A. O'Neill, Rac1 regulates interleukin 1-induced nuclear factor kappaB activation in an inhibitory protein kappaBalpha-independent manner by enhancing the ability of the p65 subunit to transactivate gene expression, J. Biol. Chem. 275 (2000) 3114–3120.
[57] A. Naldini, I. Filippi, D. Miglietta, M. Moschetta, R. Giavazzi, F. Carraro, Interleukin-1beta regulates the migratory potential of MDAMB231 breast cancer cells through the hypoxia-inducible factor-1alpha, Eur. J. Canc. 46 (2010) 3400–3408.
[58] R.N. Apte, S. Dotan, M. Elkabets, M.R. White, E. Reich, Y. Carmi, X. Song, T. Dvozkin, Y. Krelin, E. Voronov, The involvement of IL-1 in tumorigenesis, tumor invasiveness, metastasis and tumor-host interactions, Canc. Metastasis Rev. 25 (2006) 387–408.
[59] I. Kaplanov, Y. Carmi, R. Kornetsky, A. Shemesh, G.V. Shurin, M.R. Shurin, C. A. Dinarello, E. Voronov, R.N. Apte, Blocking IL-1beta reverses the immunosuppression in mouse breast cancer and synergizes with anti-PD-1 for tumor abrogation, Proc. Natl. Acad. Sci. U. S. A. 116 (2019) 1361–1369.
[60] M.C. Schmid, C.J. Avraamides, P. Foubert, Y. Shaked, S.W. Kang, R.S. Kerbel, J. A. Varner, Combined blockade of integrin-alpha4beta1 plus cytokines SDF-1alpha or IL-1beta potently inhibits tumor inflammation and growth, Canc. Res. 71 (2011) 6965–6975.
[61] T.C. Wu, K. Xu, J. Martinek, R.R. Young, R. Banchereau, J. George, J. Turner, K. I. Kim, S. Zurawski, X. Wang, D. Blankenship, H.M. Brookes, F. Marches, G. Obermoser, E. Lavecchio, M.K. Levin, S. Bae, C.H. Chung, J.L. Smith, A. M. Cepika, K.L. Oxley, G.J. Snipes, J. Banchereau, V. Pascual, J. O'Shaughnessy, A. K. Palucka, IL1 receptor antagonist controls transcriptional signature of inflammation in patients with metastatic breast cancer, Canc. Res. 78 (2018) 5243–5258.
[62] G. Biffi, T.E. Oni, B. Spielman, Y. Hao, E. Elyada, Y. Park, J. Preall, D.A. Tuveson, IL1-Induced JAK/STAT signaling is antagonized by TGFbeta to shape CAF heterogeneity in pancreatic ductal adenocarcinoma, Canc. Discov. 9 (2019) 282–301.